CHEMMEDCHEM

DOI: 10.1002/cmdc.201100578

Structure–Activity Relationships for Negative Allosteric mGluR5 Modulators

Birgitte H. Kaae,[a, b] Kasper Harpsøe,[a] Trine Kvist,[a] Jesper M. Mathiesen,[a] Christina Mølck,[a] David Gloriam,[a] Hermogenes N. Jimenez,[c] Michelle A. Uberti,[c] Søren M. Nielsen,[d] Birgitte Nielsen,[a] Hans Bräuner-Osborne,[a] Per Sauerberg,[e] Rasmus P. Clausen,*[a] and Ulf Madsen[a]

A series of compounds based on the mGluR5-selective ligand 2-methyl-6-(phenylethynyl)pyridine (MPEP) were designed and synthesized. The compounds were found to be either structural analogues of MPEP, substituted monomers, or dimeric analogues. All compounds retained mGluR5 selectivity with only weak or no activity at other mGluRs or iGluRs. The substituted analogue, 1,3-bis(pyridin-2-ylethynyl)benzene (**19**), is a potent negative modulator at mGluR5, whereas all other compounds lost potency relative to MPEP and showed that activity is highly dependent on the position of the nitrogen atom in the pyridine moieties. A homology modeling and ligand docking study was used to understand the binding mode and the observed selectivity of compound **19**.

Introduction

(*S*)-Glutamate ((*S*)-Glu, **1**; Figure 1) is the major excitatory neurotransmitter in the vertebrate central nervous system (CNS). (*S*)-Glu nonselectively activates ionotropic and metabotropic glutamate receptors (iGluRs and mGluRs).[1] The G-protein-coupled mGluRs consist of eight cloned subtypes (mGluR1–8), which are divided into three classes based on pharmacology and sequence homology. Group I includes mGluR1 and 5, Group II includes mGluR2 and 3, and Group III includes mGluR4, 6, 7, and 8. Since the first evidence for mGluRs was reported,[2] there has been an intense search for mGluR ligands that can discriminate between the eight subtypes. Ligands developed include orthosteric agonists and antagonists such as compounds **2** and **3**, and more recently positive and negative allosteric modulators such as compounds **4**–**7** (Figure 1).[1b] Such ligands may help elucidate the physiological role of mGluRs in the normal and diseased states of the mammalian brain and they have the potential for therapeutic applications.[1a,b]

Group I mGluRs are important for CNS memory, learning, and fear conditioning.[1b,3] In particular, the mGluR5 subtype has been implicated in numerous psychiatric disorders such as schizophrenia, depression, and anxiety as well as neurodegenerative diseases like Parkinson's disease.[1b,4]

Interest is growing for allosteric ligands that bind the less conserved seven-transmembrane (TM) domain of the mGluR5 protein, for the development of selective compounds. Compound **5** is a negative allosteric modulator at mGluR1, whereas compounds **6** and **7** are selective for mGluR5. Rational struc-

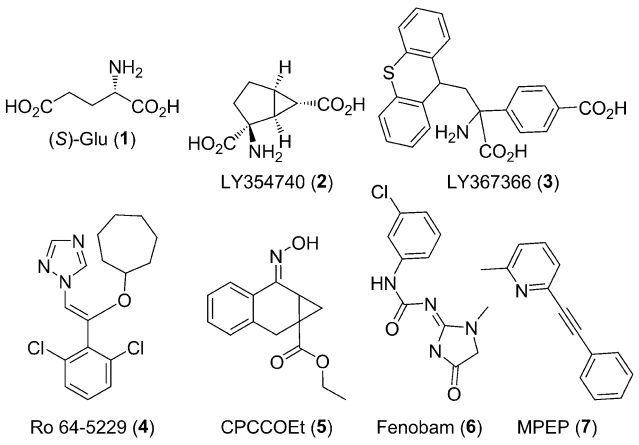

Figure 1. Examples of mGluR ligands: the endogenous ligand (*S*)-glutamate (**1**); compounds **2** and **3** are competitive ligands, and compounds **4**–**7** are allosteric modulators.

[a] *Dr. B. H. Kaae, Dr. K. Harpsøe, T. Kvist, Dr. J. M. Mathiesen, C. Mølck, Dr. D. Gloriam, B. Nielsen, Prof. H. Bräuner-Osborne, Dr. R. P. Clausen, Dr. U. Madsen*
Department of Molecular Drug Research
Faculty of Pharmaceutical Sciences, University of Copenhagen
Universitetsparken 2, 2100 Copenhagen (Denmark)
E-mail: rac@farma.ku.dk

[b] *Dr. B. H. Kaae*
Radiometer Innovation, Radiometer Medical Aps
Åkandevej 21, 2700 Brønshøj (Denmark)

[c] *H. N. Jimenez, M. A. Uberti*
ST-1 Glutamate Biology, Lundbeck Research USA
215 College Road, Paramus, NJ 07652-1431 (USA)

[d] *S. M. Nielsen*
Molecular Pharmacology, H. Lundbeck A/S
Ottiliavej 9, 2500 Valby (Denmark)

[e] *P. Sauerberg*
Diabetes Protein & Peptide Chemistry, Novo Nordisk A/S
Novo Nordisk Park 1, 2760 Måløv (Denmark)

Supporting information for this article is available on the WWW under http://dx.doi.org/10.1002/cmdc.201100578.

ture-based design of subtype-selective allosteric modulators is hampered by the lack of crystal structures that contain the membrane-spanning helices. However, published rhodopsin-based homology models[5] of mGluR5 and pharmacophores for the allosteric binding site[6] are available. Mutational studies have shown that amino acid residues in the same areas of the TM helical bundles of mGluR1 and mGluR5 are important for the binding of certain negative allosteric modulators.[6]

To investigate potency and selectivity, we decided to prepare potential mGluR ligands based on the concept of bivalent ligands. The hypothesis that the affinity of a bivalent molecule for its target is greater than the sum of its fragments was proposed by Page and Jencks in the 1970s.[7] Assuming that the translational and rotational entropy of each fragment in a symmetrical dimer equals the total translational and rotational entropy for the bivalent molecule, the loss of entropy will decrease upon joining the two fragments, leading to increased affinity. However, the dimerization of ligands has served other purposes such as improving pharmacokinetic properties, selectivity, potency, and solubility.[8]

In the present study we investigated the dimerization of 2-methyl-6-(phenylethynyl)pyridine (MPEP) analogues. Selective inhibition of mGluR5 by MPEP has proven to be neuroprotective against *N*-methyl-D-aspartate (NMDA)-induced neuronal damage,[9] and MPEP also displays anxiolytic properties.[4b] Herein we present the synthesis and pharmacological characterization of a variety of monomeric MPEP analogues, substituted monomers, and dimeric MPEP analogues. Furthermore, we carried out homology modeling and a ligand docking study to explain the observed selectivity toward mGluR5 over mGluR1.

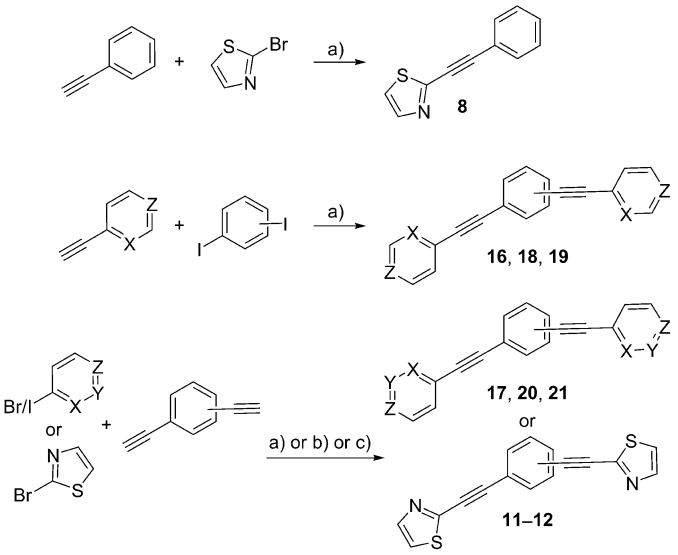

Scheme 1. Synthesis of compounds **8**, **11**–**12**, and **16**–**21** using palladium-catalyzed Sonogashira cross-couplings: a) $PdCl_2(PPh_3)_2$, CuI, Et_3N, CH_2Cl_2; **8** (96%), **11** (87%), **12** (89%), **16** (95%), **18** (87%), **19** (96%); b) $PdCl_2(PPh_3)_2$, CuI, Cs_2CO_3, DMF; **17** (97%), **20** (96%); c) $PdCl_2(PPh_3)_2$, CuI, Et_3N, THF; **21** (56%).

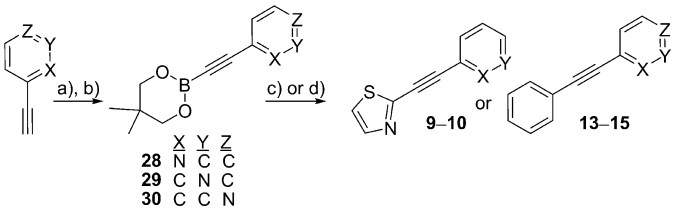

Scheme 2. Synthesis of monomeric compounds **9**–**10** and **13**–**15** using palladium-catalyzed Suzuki cross-couplings: a) Diisopropylamine, *n*BuLi, Et_2O, $B(OiPr)_3$; b) AcOH, 2,2-dimethyl-1,3-propanediol; **28** (68%), **29** (59%), **30** (58%); c) $PdCl_2(PPh_3)_2$, Cs_2CO_3, DMF; **9** (92%), 13 (95%), **14** (92%), **15** (71%); d) $PdCl_2(PPh_3)_2$, Cs_2CO_3, DME, H_2O; **10** (89%).

Results and Discussion

Chemistry

Compounds **8**, **11**, **12**, and **16**–**21** (Figure 2) were synthesized according to Scheme 1 using palladium(0)-catalyzed Sonogashira cross-coupling reactions. The reactions were optimized by using different bases and solvents. The electronic properties of the electrophile, nucleophile, and palladium catalyst were used to optimize and increase the yield of the reactions. In general, $PdCl_2(PPh_3)_2$-catalyzed reactions had fewer by-products and gave higher yields than any of the other tested catalysts. Not surprisingly, the choice of nucleophile and electrophile greatly influenced the outcome too. The Sonogashira cross-coupling reactions are very sensitive to atmosphere and care should be taken to minimize the formation of homocoupled by-products, which severely complicates the purification of compounds **16**–**21**. Three by-products **43**–**45** (Figure 3) were obtained in fairly large amounts and were isolated and tested for pharmacological activity as well.

Monomeric compounds **9**, **10**, and **13**–**15** (Figure 2) were synthesized by palladium-catalyzed Suzuki cross-coupling reactions according to Scheme 2. In general, crude compounds **28**–**30** could be used for the subsequent cross-coupling reactions.

The dimeric analogues **22**–**27** of compounds **13**–**15** were synthesized similarly by Suzuki cross-coupling reactions (Scheme 3). The halogenated analogues **31**–**36** were purified and metalated to generate the boronic esters **37**–**42**, which were used for the Suzuki cross-coupling reactions.

Pharmacology

All compounds depicted in Figures 2 and 3 were pharmacologically characterized on Group I mGluR1 and mGluR5, Group II mGluR2, and Group III mGluR4 with respect to allosteric modulation. Characterization at mGluR1 was performed by an inositol phosphate (IP) turnover assay with CHO cells expressing mGluR1.[10] Compounds **19**–**21**, however, were assayed by measurement of intracellular Ca^{2+} concentrations essentially as described for mGluR5 below. CHO cells expressing mGluR2 or mGluR4[11] were employed for characterization on mGluR Groups II and III, respectively. The activity was measured as inhibition of forskolin-stimulated cAMP production. We have pre-

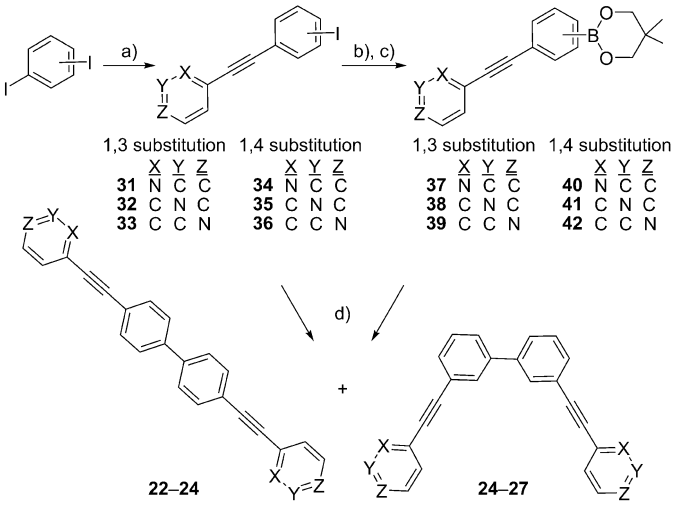

Scheme 3. Synthesis of dimeric compounds **22**–**27** using palladium-catalyzed Suzuki cross-couplings: a) $PdCl_2(PPh_3)_2$, CuI, Et_3N, CH_2Cl_2; **31** (81%), **32** (82%), **33** (78%), **34** (57%), **35** (32%), **36** (63%); b) *n*BuLi, Et_2O, $B(OiPr)_3$ c) AcOH, 2,2-dimethyl-1,3-propanediol; **37** (91%), **38** (96%), **39** (81%), **40** (99%), **41** (98%), **42** (84%); d) $PdCl_2(PPh_3)_2$, K_2CO_3, PPh_3, 1,4-dioxane, H_2O; **22** (62%), **23** (85%), **24** (78%), **25** (72%), **26** (66%), **27** (88%).

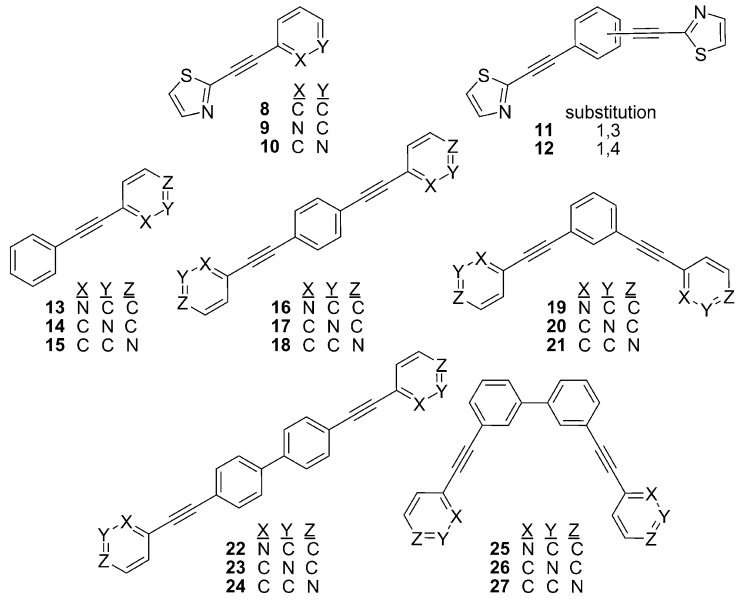

Figure 2. Synthesized and characterized compounds **8**–**27**. Two series were investigated: those containing 1) thiazoles and 2) pyridines. In general, series 2 displayed better solubility than series 1. The pharmacological profiles are similar, and series 2 was chosen based on solubility.

viously shown that MPEP is a weak positive allosteric modulator at mGluR4,[12a] and therefore all compounds were also evaluated for positive allosteric modulatory effects. Activity at mGluR5 was evaluated by measuring changes in intracellular Ca^{2+} concentrations in cells expressing human mGluR5, using a Ca^{2+}-sensitive fluorescent dye and a fluorescence image plate reader (FLIPR). All compounds **8**–**27** and **43**–**45** depicted in Figure 2 and Figure 3 were tested for agonist, antagonist, negative, or positive modulator activity on mGluR1, mGluR2, mGluR4, and mGluR5. Furthermore, the compounds were characterized pharmacologically at native iGluRs on rat cortical membranes using [^{3}H]AMPA, [^{3}H]KA and [^{3}H]CGP39653 binding assays,[13] representing 2-amino-3-(5-methyl-3-oxo-1,2-oxazol-4-yl)propanoic acid (AMPA), kainic acid (KA), and NMDA receptors, respectively. No significant affinity was observed for any of the compounds in the assays representing iGluRs. Data obtained at mGluRs are listed in Table 1.

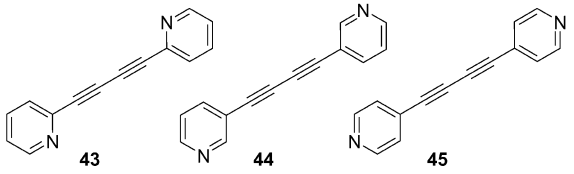

Figure 3. Isolated and characterized homodimeric by-products **43**–**45**.

All compounds were devoid of agonist activity at mGluR1, 2, 4, and 5 at 100 μM, except for compound **19**, which, interestingly, is a weak agonist at mGluR4 (Table 1). All compounds were also inactive as antagonists at 100 μM toward mGluR2 (data not listed). A few compounds displayed weak antagonist activity at mGluR1. Some compounds displayed positive allosteric modulatory effects at mGluR4, which, however, was no stronger than the weak effect of MPEP[12a] and thus not characterized further. In general, the compounds maintained selectivity toward mGluR5. However, the compounds vary significantly and are very sensitive to the placements of heteroatoms. This is clearly demonstrated in comparing compounds **19**, **20**, and **21**, with activities spanning almost two orders of magnitude at mGluR5. The thiazolyl MPEP analogues generally showed much weaker potency than MPEP. However, compounds **11** and **12** were equipotent to corresponding MPEP analogues. Among the pyridines, the 2-pyridyl analogues showed the highest potency, with compounds **13**, **16**, **19**, **22**, and **25** being the most potent. Overall, the bent structures, compounds **19**–**21** and **25**–**27**, had higher potency than their linear analogues, compounds **16**–**18** and **22**–**24**. In general, all potencies were lower than that of MPEP, except for compound **19**, which is equipotent.

The homocoupled pyridine-containing by-products **43**–**45** were also characterized pharmacologically and showed only weak or no effects at mGluR5 and other mGluRs. Interestingly, by-product **44** showed agonist activity at mGluR5 as the only compound in the series.

Homology model of mGluR5 and putative binding mode of compound 19

We constructed a homology model of the mGluR5 TM helical bundle based on the human β2-adrenergic receptor co-crystallized with an inverse agonist (PDB ID: 2RH1[14]) and the human A_{2A} adenosine receptor in complex with an antagonist (PDB ID:

Table 1. Pharmacological characterization of compounds **8**–**27** and **43**–**45**.

Compd	mGluR1 IC_{50} [μM] ($pIC_{50}\pm$SEM)	mGluR4 MPEP effect [%][a]	mGluR5 IC_{50} [μM] ($pIC_{50}\pm$SEM)	mGluR5 EC_{50} [μM] ($pEC_{50}\pm$SEM)
MPEP	>100	100±4.7	0.00099	>100
8	>100	77.0±12.5	0.25 (6.6±0.00)	>100
9	>100	−14±13.3	1.37 (5.9±0.06)	>100
10	>100	−17.8±11.8	2.33 (5.7±0.17)	>100
11	>100	−0.9±16.3	0.026 (7.7±0.22)	>100
12	>100	16.5±13.9	0.017 (7.8±0.02)	>100
13	>100	75.6±12.3	0.021 (7.7±0.16)	>100
14	>100	109±6.9	0.13 (6.9±0.15)	>100
15	160 (3.8±0.03)	134.2±3.3	0.68 (6.2±0.08)	>100
16	>100	73.9±14.5	0.026 (7.7±0.23)	>100
17	>100	69.6±12.4	1.06 (6.0±0.01)	>100
18	>100	21.6±15.4	0.99 (6.1±0.04)	>100
19	25 (4.6±0.09)	61.0±12.0[b]	0.00083 (9.0±0.05)	>10
20	>100	43.0±15.0	0.250 (6.6±0.1)	>10
21	>100	64.0±9.0	0.070 (7.2±0.2)	>10
22	81 (4.1±0.02)	41.0±2.7	0.24 (6.6±0.05)	>100
23	>100	41.6±2.7	>100	>100
24	>100	46.8±10.1	1.04 (6.0±0.04)	>100
25	6.4 (5.2±0.02)	47.5±7.9	0.029 (7.5±0.01)	>100
26	28 (4.6±0.20)	93.7±8.1	1.35 (5.9±0.01)	>100
27	>100	26.6±14.7	0.10 (7.1±0.33)	>100
43	78 (4.1±0.08)	−9.0±10.4	0.16 (6.8±0.16)	>100
44	>100	−3.9±9.9	>100	0.46 (6.4±0.11)
45	>100	−14.2±10.2	>100	>100

[a] Determined with MPEP at 100 μM; values represent the mean ±SEM. [b] EC_{50} [μM] ($pEC_{50}\pm$SEM): 25 (4.6±0.1).

3EML[15]). Both structures correspond to an inactive receptor state,[16] and negative modulators are proposed to act by stabilizing the inactive conformation, opposing activation.[5a] Like many other GPCRs, mGluR5 was found to contain a cavity between the upper halves of the seven TM helices that also correspond to the ligand binding sites of the two templates. Distant homology models must be interpreted with great care in the generation of binding mode and SAR hypotheses. Mapping corresponding residues that have been previously shown to be important for binding of a negative modulator in rat

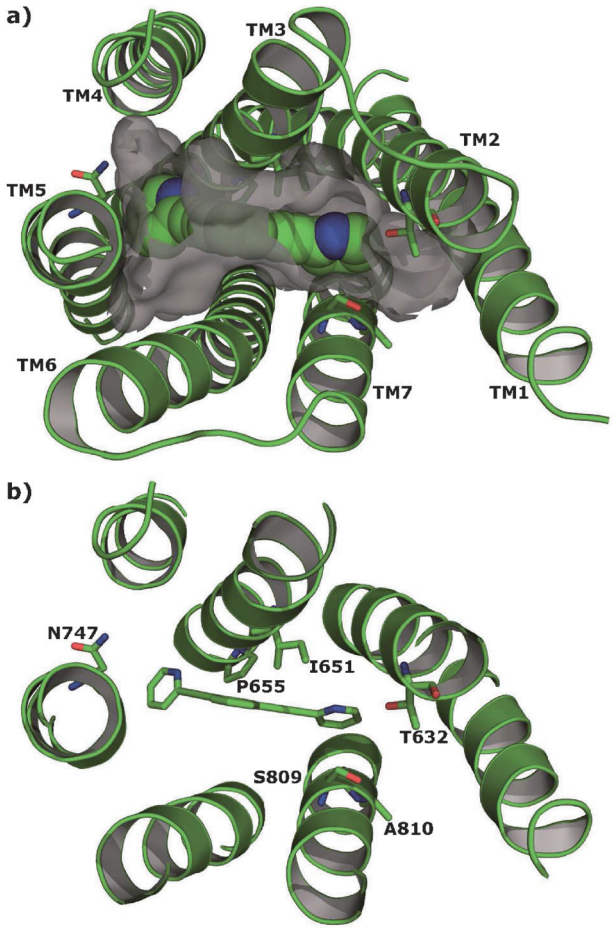

Figure 4. Representations of the mGluR5 homology model with compound **19** docked into the putative binding site. a) The binding site is represented as a grey transparent Connolly surface, and **19** is represented as spheres to show the shape complementarity. b) Same view as above with truncated helices and without the surface and spheres to more clearly show the relative location of the residues discussed in the text. Residues Thr632$^{2.61}$, Ile651$^{3.32}$, Pro655$^{3.36}$, Asn747$^{5.46}$, Ser809$^{7.39}$, and Ala810$^{7.40}$ are shown as sticks. The image was created in PyMOL.[18]

mGluR5[5a] indicates that this is indeed the site of action. Thus, to get an estimate of the binding site we docked compound **19** to the mGluR5 homology model and observed a pocket with a Connolly surface that closely complements the shape of **19** (Figure 4a). The rigid nature of **19** and the shape complementarity render this a likely binding mode, and the lack of hydrogen bonds to the receptor may be solved by refinement of the model, as potential interaction partners, Thr632$^{2.61}$, Asn747$^{5.46}$, and Ser809$^{7.39}$ are found in the vicinity of the two pyridine rings (Figure 4b).

mGluR5 selectivity of compound 19

To find a structural rationale that explains the selectivity of **19** for mGluR5 over mGluR1, we investigated the modulator binding site defined as all residues located within 5 Å of the docked **19** and with side chains pointing toward the modulator. A comparison of the binding site residues at the sequence level (Figure 5) shows that only four residues differ in mGluR5:

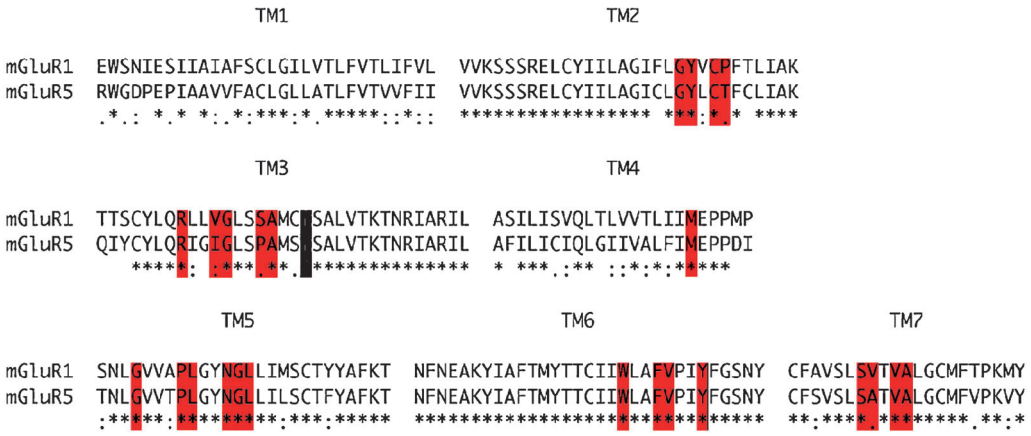

Figure 5. Sequence alignment of the TM helices of mGluR1 and mGluR5. The red background highlights the residues of the modulator binding site defined as residues located within 5 Å of the suggested binding mode of compound **19** and side chains pointing toward the modulator.

Thr 632$^{2.61}$, Ile 651$^{3.32}$, Pro 655$^{3.36}$, and Ala 810$^{7.40}$. In fact, the residues corresponding to Pro 655$^{3.36}$ and Ala 810$^{7.40}$ in rat mGluR5 have been shown to be important for binding and function of the negative modulator, MPEP.[5a,17] In our binding model the side chain of Ala 810$^{7.40}$ points toward TM1 (Figure 4b), but allowing a small rotation of helix 7 would bring it into a position where a valine, as in mGluR1, would sterically interfere with the modulator. Ile 651$^{3.32}$ is in close van der Waals contact to **19** in our model, but the conservative change to the corresponding valine in mGluR1 is not expected to significantly alter the binding site to result in mGluR5 selectivity. Thr 632$^{2.61}$ and Pro 655$^{3.36}$ both take part in shaping the binding site and correspond respectively to proline and serine residues in mGluR1. This represents a significant difference in the local environment of the binding site from hydrophilic to hydrophobic and vice versa, which may likely impact modulator binding and function.

Based on our binding model we predict that Thr 632$^{2.61}$, Pro 655$^{3.36}$, and/or Ala 810$^{7.40}$ could be responsible for the selectivity of **19** for mGluR5 over mGluR1. In support of this, Pagano et al. showed previously that Pro 655$^{3.36}$, Ser 658$^{3.39}$, and Ala 810$^{7.40}$ are involved in MPEP selectivity between mGluR1 and mGluR5,[17] indicating an overlap of binding sites for MPEP and **19**. Due to differences in binding mode, Ser 658$^{3.39}$ is not predicted to be involved in the binding and selectivity of **19**, but this may be the case for those compounds that are similar in size to MPEP, such as compound **15**. In addition, residues from the second extracellular loop (ECL2) could contribute to the observed selectivity for all compounds presented herein.

Conclusions

We have designed and synthesized a series of ligands based on the selective mGluR5 negative modulator, MPEP. The compounds are either structural analogues of MPEP, substituted monomers, or dimeric analogues. This led to the potent mGluR5-selective compound **19**. All other compounds are less potent than MPEP and showed that the activity is highly dependent on the position of the nitrogen heteroatom in the pyridine moieties, with 2-pyridyl having the highest activity. The bent analogues have greater activity than their linear counterparts. All compounds retain mGluR5 selectivity with only weak or no activity at other mGluRs or iGluRs.

In combination with the sequence alignment (Figure 5), our mGluR5 homology model indicates that as few as three residues may be responsible for the differences in modulator IC_{50} values between mGluR1 and mGluR5. This has provided further insight into the binding mode of mGluR5-modulatory agents and gives directions for the future design of selective compounds.

Experimental Section

Chemistry

All reactions involving air-sensitive reagents were performed under an atmosphere of N_2. Et_2O was distilled and stored over Na. THF was freshly distilled from Na/benzophenone under N_2. $Pd(PPh_3)_4$ was freshly prepared.[19] $ZnCl_2$ was flame-dried in vacuo. Commercially available *n*BuLi and Grignard reagents were titrated prior to reaction.[20] Column chromatography (CC) was performed using Merck silica (0.063–0.200 mm), whereas Merck silica (0.035–0.070 mm) or silica 60A (20–45 μm) were used for flash chromatography (FC) and columns for CombiFlash purification (CF). Compounds were visualized on TLC plates (Merck silica gel 60 F_{254}) using UV light, $KMnO_4$, or CeMo spraying reagents. Melting points were measured on a Büchi melting point B-545 apparatus or on an SRS Optimelt apparatus in open capillaries and are uncorrected.

^{1}H NMR (300 MHz) and ^{13}C NMR (75 MHz) spectra were recorded on a Varian Gemini spectrometer, a Varian Mercury spectrometer, or on a Bruker DRX-300 instrument. ^{1}H NMR (400 MHz), ^{13}C NMR (100 MHz), COSY and Fluoro-Eretic spectra were recorded on a Bruker DRX-400 instrument. When $CDCl_3$ was employed as solvent TMS or $CDCl_3$ were used as internal standards. For other solvents the solvent residual peak was used as internal standard. Chemical shifts (δ) are expressed in ppm and coupling constants (J) in hertz.

GC–MS was performed on either a Shimadzu QP5050A instrument using EI or CI, or on an Agilent 6890 GC system connected to an Agilent 5973 network mass-selective detector using EI, API-ES+, or

CI. GC was carried out by direct inlet on a Chrompack gas chromatograph CP 9001 system.

Analytical HPLC was performed on one of the following systems: 1) An HPLC system consisting of a Jasco 880 pump, a Rheodyne 7125 injector equipped with a 100 μL Rheodyne loop, a TSP AS3000 autosampler, and a TSP UV100 detector set at the desired wavelength. The system was controlled by a computer using TSP PC100 software.

2) An HPLC system consisting of a Dionex Ultimate 3000 pump, a Rheodyne 7125 injector equipped with a 100 μL Rheodyne loop, a TSP AS3000 autosampler, and a Dionex Ultimate 3000 photodiode array detector set at the desired wavelength. The system was controlled by a computer using Chromeleon version 6.80.

3) A Gilson HPLC system consisting of a 402 syringe pump (500 μL), and a 234 autoinjector. The flow was maintained at 0.7–1.5 mL min^{-1}, depending on the column, by two 306 pumps connected to an 811c dynamic mixer, of which one was via an 805 manometric module. Four valvemates secured injection of sample onto the desired column. Signals were detected by a UV/Vis 155 detector. The system was controlled by a computer using Unipoint version 3.30.

A number of columns were used: Waters Xterra MS C_{18} (50 mm × 3 mm, 5 μm), Supelcosil Lichrosorb SI-60 (150 mm × 3.2 mm, 5 μm), Kromasil SI-60 (250 mm × 4.6 mm, 10 μm), one of the following Phenomenex columns: Luna C_{18} (150 mm × 4.6 mm, 5 μm), Gemini C_6-phenyl 110 (50 mm × 3 mm, 5 μm).

Preparative HPLC was carried out on a Gilson HPLC system consisting of a 5 mL Rheodyne loop, a 215 liquid handler, and an 819 injection valve actuator connected to the column via a prime/purge valve and a injection valve. The flow was maintained between 7 and 50 mL min^{-1}, depending on the column, by four 306 pumps connected (one via an 806 manometric module) to an 811c dynamic mixer. A UV/Vis 155 detector and a fraction collector secured collection of fractions. The system was controlled by a computer using Unipoint version 3.30.

Analytical LC–MS was carried out on an Agilent 1100 apparatus consisting of a gradient pump, an isocratic pump 3, a 1100 diode array detector, and a mass spectrometer, a 1100 valve 1 G1160A 12 ps 13 pt, a 1100 valve 2 G1158 2 ps 6 pt, an analog digital converter, and a 1100 dual-loop autosampler ps1. One of the following columns was used: Supelcosil Lichrosorb SI-60 (150 mm × 3.2 mm, 5 μm), Waters Xterra MS C_{18} (50 mm × 3.0 mm, 5 μm), Phenomenex Luna (150 mm × 4.6 mm, 5 μm), or Phenomenex Gemini C_6-phenyl 110 (50 mm × 3 mm, 5 μm). Fractions were reported on the basis of either UV or MS (*M*, *M* + 1, or *M* + 23).

Preparative LC–MS was performed on an Agilent 1100 apparatus consisting of a gradient preparative pump, an isocratic pump 3, a 1100 diode array detector, and a mass spectrometer, a 1100 valve 1 G1160A 12 ps 13 pt, a 1100 valve 2 G1158 2 ps 6 pt, an analog digital converter, a 1100 dual-loop autosampler ps1, and four 1100 fraction collectors. Fractions were collected on the basis of either UV or MS (*M*, *M* + 1, or *M* + 23).

HRMS was performed at the Mass Spectrometry Research Unit, Department of Chemistry, University of Copenhagen, Denmark. Microanalyses of tested compounds agree with theoretical values ±0.4%, and were carried out at the Analytical Research Department, H. Lundbeck A/S, Denmark; at Mikroanalytisk Afd. by Birgitta Kegel, Department of Chemistry, University of Copenhagen; by Mikro Kemi AB, Seminariegatan, Uppsala, Sweden; or by J. Theiner, Department of Physical Chemistry, University of Vienna, Austria.

2-(Phenylethynyl)thiazole (8): 2-Bromothiazole (1.78 mL, 20 mmol) was dissolved in dry CH_2Cl_2 (40 mL). CuI (40 mg, 0.2 mmol), $PdCl_2(PPh_3)_2$ (145 mg, 0.2 mmol), Et_3N (20 mL), and phenylacetylene (3.29 mL, 30 mmol) were added, and the reaction mixture was heated at reflux for 5 h. The mixture was diluted with Et_2O (60 mL), filtered and evaporated. FC (CH_2Cl_2/MeOH gradient (0–5%)) afforded **8** as a red–brown oil, which was further purified by Kugel Rohr distillation (2.8 mbar, 155 °C) to yield the target compound as a yellow oil that crystallizes upon standing (3.56 g, 19.2 mmol, 96%); mp: < 35 °C; ^{1}H NMR ($CDCl_3$): δ = 7.33–7.41 (m, 4H), 7.61 (m, 2H), 7.87 ppm (d, *J* = 3.23 Hz, 1H); ^{13}C NMR ($CDCl_3$): δ = 82.70, 91.50, 121.44, 123.23, 130.00, 130.23, 131.85, 137.29, 144.10 ppm; Anal. CHN for $C_{11}H_7NS$.

2-(Pyridin-2-ylethynyl)thiazole (9): 2-Bromothiazole (0.05 mL, 0.5 mmol) was dissolved in DMF (2 mL) and $PdCl_2(PPh_3)_2$ (17 mg, 0.03 mmol) was added. The mixture was stirred for 15 min at RT before the addition of **28** (161 mg, 0.75 mmol), Cs_2CO_3 (489 mg, 1.5 mmol) and DMF (2 mL). The reaction mixture was heated at 80 °C for 5 h. H_2O (15 mL) and EtOAc (15 mL) were added and the phases separated. The aqueous phase was further extracted with EtOAc (2 × 10 mL). The combined organic phases were washed with H_2O (5 mL), 1 M NaOH (2 × 10 mL) and H_2O (10 mL), and afterward dried (Na_2SO_4). Evaporation afforded crude **9**. FC (CH_2Cl_2/Et_3N (5%)/MeOH gradient (0–5%)) gave **9** as brown crystals, which were dried in vacuo (86 mg, 92%); mp: 72.4–73.3 °C; ^{1}H NMR ($CDCl_3$/TMS): δ = 7.32 (ddd, *J* = 2.0, 4.5, 7.5 Hz, 1H), 7.45 (d, *J* = 3.5 Hz, 1H), 7.62 (td, *J* = 1.2, 6.0 Hz, 1H), 7.73 (dt, *J* = 3.0, 7.5 Hz, 1H), 7.91 (d, *J* = 3.5 Hz, 1H), 8.66 ppm (d, *J* = 7.5 Hz, 1H); ^{13}C NMR ($CDCl_3$/TMS): δ = 81.5, 92.4, 121.7, 123.8, 127.8, 136.4, 142.0, 143.9, 149.9, 150.4 ppm; MS (EI) 186; Anal. CHN for $C_{10}H_6N_2S$.

2-(Pyridin-3-ylethynyl)thiazole (10): 2-Bromothiazole (0.05 mL, 0.5 mmol) was dissolved in DME (2 mL) and $PdCl_2(PPh_3)_2$ (17 mg, 0.03 mmol) was added. The mixture was stirred for 15 min at RT before the addition of **29** (161 mg, 0.75 mmol), Cs_2CO_3 (489 mg, 1.5 mmol) and H_2O (2 mL). The reaction mixture was heated at 80 °C for 14 h. H_2O (15 mL) and EtOAc (15 mL) were added and the phases separated. The aqueous phase was further extracted with EtOAc (2 × 10 mL). The combined organic phases were washed with H_2O (5 mL), 1 M NaOH (2 × 10 mL) and H_2O (10 mL), and afterward dried (Na_2SO_4). Evaporation afforded crude **10**. Preparative HPLC (H_2O/MeCN gradient/0.1% TFA) using a Luna column C_{18}(2) (250 mm × 21.2 mm, 5 μm) yielded **10**. TFA residing from LC–MS was removed by dissolving **10** in MeOH and run through a SPE-PL-HCO_3 (MP) tube. Compound **10** was obtained as red–brown crystals, which were dried in vacuo (82 mg, 89%); mp > 200 °C (dec); ^{1}H NMR ($CDCl_3$/TMS): δ = 7.34 (dd, *J* = 2.8, 6.1 Hz, 1H), 7.44 (d, *J* = 6.9 Hz, 1H), 7.85–7.92 (m, 2H), 8.62 (d, *J* = 6.2 Hz, 1H), 8.84 ppm (d, *J* = 0.8 Hz, 1H); ^{13}C NMR ($CDCl_3$/TMS): δ = 76.6, 87.3, 121.7, 123.0, 126.0, 143.4, 143.8, 145.0, 146.6, 160.2 ppm; Anal. CHN for $C_{10}H_6N_2S$.

1,3-Bis(thiazol-2-ylethynyl)benzene (11): 2-Bromothiazole (0.90 mL, 10 mmol) was dissolved in dry CH_2Cl_2 (20 mL). CuI (20 mg, 0.1 mmol), $PdCl_2(PPh_3)_2$ (75 mg, 0.1 mmol), Et_3N (10 mL), and 1,3-diethynylbenzene (0.90 mL, 6.8 mmol) were added, and the reaction mixture was held at reflux for three days. The mixture was diluted with Et_2O (50 mL), filtered and evaporated. CC using CH_2Cl_2/MeOH gradient (0–5%) afforded **11** as light-brown crystals, which were recrystallized from EtOAc/heptane (1.34 g, 92%); mp: 110.2–114.6 °C (dec). Preparative HPLC (H_2O/MeCN gradient/0.1%

TFA) using a Luna $C_{18}(2)$ column (250×21.2 mm, 5 μm) gave **11**. TFA residing from HPLC was removed by dissolving **11** in MeOH and run through a SPE-PL-HCO_3 (MP) tube. Compound **11** was obtained as off-white powder-like crystals, (1.27 g, 87%); mp: 113.8–115.2 °C (dec); ^{1}H NMR ($CDCl_3$/TMS): δ = 7.48 (t, J = 7.0 Hz, 1H), 7.55 (d, J = 3.2 Hz, 2H), 7.68 (d, J = 7.0 Hz, 2H), 7.87 (s, 1H), 8.05 ppm (d, J = 3.2 Hz, 2H); ^{13}C NMR ($CDCl_3$/TMS): δ = 83.1, 92.5, 121.1, 122.3, 128.9, 132.8, 135.0, 143.8, 148.4; Anal. CHN for $C_{16}H_8N_2S_2$.

1,4-Bis(thiazol-2-ylethynyl)benzene (12): 2-Bromothiazole (0.90 mL, 10 mmol) was dissolved in dry CH_2Cl_2 (20 mL). CuI (20 mg, 0.1 mmol), $PdCl_2(PPh_3)_2$ (75 mg, 0.1 mmol), Et_3N (10 mL), and 1,4-diethynylbenzene (0.90 mL, 7.0 mmol) were added, and the reaction mixture was held at reflux for three days. The mixture was diluted with Et_2O (65 mL), filtered and evaporated. FC using CH_2Cl_2/MeOH gradient (0–5%) afforded **12**. Compound **12** was dried in vacuo and obtained as brown crystals (1.33 g, 91%); mp: 189–193 °C (dec). HPLC (heptane/EtOH gradient) using a Supelcosil LC-SI column (250 mm×21.2 mm, 5 μm) yielded **12**, as yellow crystals (1.29 g, 89%); mp: 191–193 °C; ^{1}H NMR ($CDCl_3$/TMS): δ = 7.44 (d, J = 3.9 Hz, 2H), 7.59 (s, 4H), 7.89 ppm (d, J = 3.9 Hz, 2H); ^{13}C NMR ($CDCl_3$/TMS): δ = 84.5, 93.1, 121.2, 122.5, 132.0, 143.8, 148.4; MS (EI) 292.0 ppm $[M]^+$; Anal. CHN for $C_{16}H_8N_2S_2 \cdot {}^1/_3\,H_2O$.

2-(Phenylethynyl)pyridyl (13): Iodobenzene (0.06 mL, 102 mg, 0.6 mmol) was dissolved in DMF (2 mL) and $PdCl_2(PPh_3)_2$ (17 mg, 0.025 mmol) was added. The mixture was stirred for 15 min at RT before the addition of **28** (161 mg, 0.75 mmol) Cs_2CO_3 (489 mg, 1.5 mmol) and DMF (2 mL). The reaction mixture was heated at 80 °C for 3 h. H_2O (15 mL) and EtOAc (15 mL) were added and the phases separated. The aqueous phase was further extracted with EtOAc (2×10 mL). The combined organic phases were washed with H_2O (5 mL), 1 M NaOH (2×10 mL) and H_2O (10 mL) and afterward dried (Na_2SO_4). Evaporation afforded crude **13**. Preparative LC–MS (H_2O (0.1% TFA)/MeCN gradient) using a Waters Xterra Prep RP_{18} column (150 mm×30 mm, 10 μm) afforded **13** when fractions were collected on the basis of m/z = 179. TFA residing from LC–MS was removed by dissolving **13** in MeOH and run through a SPE-PL-HCO_3 (MP) tube. Compound **13** was dried in vacuo, (85 mg, 95%); ^{1}H NMR ($CDCl_3$/TMS): δ = 7.20 (t, J = 7.0 Hz, 1H), 7.33–7.36 (m, 3H), 7.51 (d, J = 7.5 Hz, 1H), 7.59–7.67 (m, 3H), 8.61 ppm (d, J = 7.0 Hz, 1H); ^{13}C NMR ($CDCl_3$/TMS): δ = 88.6, 89.2, 122.2, 122.8, 127.1, 128.4, 128.8, 132.0, 136.2, 143.4, 150.0 ppm; MS (API-ES+) 180.1 $[M+1]^+$; Anal. CHN for $C_{13}H_9N$.

3-(Phenylethynyl)pyridyl (14): Iodobenzene (0.06 mL, 0.6 mmol) was dissolved in DMF (2 mL) and $PdCl_2(PPh_3)_2$ (17 mg, 0.03 mmol) was added. The mixture was stirred for 15 min at RT before the addition of **29** (161 mg, 0.75 mmol), Cs_2CO_3 (489 mg, 1.5 mmol) and DMF (2 mL). The reaction mixture was heated at 80 °C for 5 h. H_2O (15 mL) and Et_2O (15 mL) were added and the phases separated. The aqueous phase was further extracted with Et_2O (2×10 mL). The combined organic phases were washed with H_2O (5 mL), 1 M NaOH (10 mL), and H_2O (10 mL) and afterward dried (Na_2SO_4). Evaporation afforded crude **14** Preparative HPLC (H_2O/MeCN gradient (0–10%)/0.1% TFA) using a Phenomenex Gemini C_6-phenyl 110A (250 mm×30 mm, 5 μm) afforded **14** as light-brown crystals. TFA residing from HPLC was removed by dissolving **14** in MeOH and run through a SPE-PL-HCO_3 (MP) tube. Evaporation afforded **14** which was dried in vacuo (82 mg, 92%); ^{1}H NMR ($CDCl_3$/TMS): δ = 7.25 (t, J = 8 Hz, 1H), 7.34–7.38 (m, 3H), 7.51–7.57 (m, 2H), 7.76 (d, J = 8 Hz, 1H), 8.54 (d, J = 5 Hz, 1H), 8.75 ppm (s, 1H); ^{13}C NMR ($CDCl_3$): δ = 84.9, 88.8, 121.0 122.9, 127.1, 128.4, 128.7, 133.5, 139.3, 148.0, 149.7 ppm; MS (API-ES+) 180.1 $[M+1]^+$; Anal. CHN for $C_{13}H_9N$.

4-(Phenylethynyl)pyridyl (15): Iodobenzene (0.22 mL, 2.0 mmol) was dissolved in DMF (5 mL) and $PdCl_2(PPh_3)_2$ (27 mg, 0.04 mmol) was added. The mixture was stirred for 15 min before the addition of **30** (633 mg, 2.9 mmol), Cs_2CO_3 (2.24 g, 6.9 mmol) and DMF (5 mL). The reaction mixture was heated at 50 °C for 72 h. H_2O (50 mL) and EtOAc (50 mL) were added and the phases separated. The aqueous phase was further extracted with EtOAc (2×30 mL). The combined organic phases were washed with H_2O (25 mL), 1 M NaOH (20 mL), and H_2O (20 mL). Drying (Na_2SO_4) and evaporation afforded crude **15**. Preparative LC–MS (H_2O (0.1% TFA)/MeCN gradient) using a Waters Xterra Prep RP_{18} column (150 mm×30 mm, 10 μm) afforded **15** when fractions were collected on the basis of m/z = 179. TFA residing from LC–MS was removed by dissolving **15** in MeOH and run through a SPE-PL-HCO_3 (MP) tube. Compound **15** was dried in vacuo (249 mg, 71%); ^{1}H NMR (CD_3CN): δ = 7.48–7.57 (m, 3H), 7.69 (td, J = 0.9, 4.4 Hz, 2H), 7.83 (d, J = 7.4 Hz, 2H), 8.72 ppm (d, J = 7.3 Hz, 2H); ^{13}C NMR ($CDCl_3$/TMS): δ = 77.7, 88.3, 124.0, 130.9, 131.8, 133.5, 135.2, 141.8, 147.3 ppm; HRMS (ESP+) calcd: 180.0813 ($C_{13}H_{10}N$ $M+1$), found: 180.0817; Anal. CHN for $C_{13}H_9N$.

1,4-Bis(pyridin-2-ylethynyl)benzene (16): $PdCl_2(PPh_3)_2$ (319 mg, 0.46 mmol) and CuI (87 mg, 0.46 mmol) were suspended in dry CH_2Cl_2 (75 mL) and 1,4-diiodobenzene (3.0 g, 9.1 mmol) was added. The mixture was stirred for 5 min at RT before the addition of 2-ethynylpyridine (2.39 mL, 23.6 mmol) and Et_3N (75 mL). The reaction mixture was stirred overnight at RT and terminated by evaporation to dryness. CF with a heptane/EtOAc gradient afforded **16** as dark-red crystals that turn dark brown overnight (2.52 g, 99%). Preparative HPLC (H_2O/MeCN gradient/0.1% TFA) using a Waters Xterra Prep RP_{18} (150 mm×30 mm, 10 μm) gave **16** as light-brown crystals, which were dried in vacuo (2.42 g, 95%); mp > 200 °C (dec); ^{1}H NMR (CD_3CN): δ = 7.76 (s, 4H), 7.79 (t, J = 7.1 Hz, 2H), 7.96 (d, J = 7.5 Hz, 2H), 8.30 (dt, J = 1.7, 8.1 Hz, 2H), 8.77 ppm (d, J = 4.1 Hz, 2H); ^{13}C NMR ([D$_6$]DMSO): δ = 72.5, 73.5, 120.7, 124.3, 130.6, 135.6, 139.8, 144.9, 148.7 ppm; MS (CI) 280; HRMS (ESP+) calcd: 281.1079 ($C_{20}H_{13}N_2$ $M+1$), found: 281.1070; Anal. CHN for $C_{20}H_{12}N_2 \cdot 3\,TFA \cdot 1.8\,H_2O$.

1,4-Bis(pyridin-3-ylethynyl)benzene (17): 1,4-Diethynylbenzene (300 mg, 2.4 mmol), 3-iodopyridine (1.71 g, 8.3 mmol), $PdCl_2(PPh_3)_2$ (33 mg, 0.05 mmol), Cs_2CO_3 (2.71 g, 8.35 mmol), and CuI (23 mg, 0.12 mmol) were suspended in dry DMF (6 mL) and the reaction mixture was stirred at 50 °C for two days. H_2O (30 mL) and EtOAc (50 mL) were added and the phases separated. The aqueous phase was further extracted with EtOAc (2×30 mL). The combined organic phases were washed with H_2O (30 mL), 1 M NaOH (2×30 mL), and H_2O (30 mL). Drying (Na_2SO_4) and evaporation afforded crude **17**. Preparative HPLC (H_2O/MeCN gradient (0–18%)/0.1% TFA) using a Luna $C_{18}(2)$ column (250 mm×21.2 mm, 5 μm) gave **17**. TFA residing from HPLC was removed by dissolving **17** in MeOH and run through a SPE-PL-HCO_3 (MP) tube. Compound **17** was obtained as brown crystals (647 mg, 97%); mp: 191.3–191.7 °C; ^{1}H NMR ($CDCl_3$/TMS): δ = 7.28–7.32 (dd, J = 5.1, 7.9 Hz, 2H), 7.57 (s, 4H), 7.84 (d, J = 8.0 Hz, 2H), 8.58 (d, J = 5.2 Hz, 2H), 8.79 ppm (s, 2H); ^{13}C NMR ($CDCl_3$/TMS): δ = 88.0, 92.1, 120.2, 122.9, 123.1, 131.7, 138.5, 148.8, 152.3 ppm; MS (EI) 280; Anal. CHN for $C_{20}H_{12}N_2$.

1,4-Bis(pyridin-4-ylethynyl)benzene (18): $PdCl_2(PPh_3)_2$ (319 mg, 0.46 mmol) and CuI (87 mg, 0.46 mmol) were suspended in dry CH_2Cl_2 (75 mL) and 1,4-diiodobenzene (3.0 g, 9.1 mmol) was added. The mixture was stirred for 5 min at RT before the addition of 4-ethynylpyridine hydrochloride (2.63 g, 18.8 mmol) and Et_3N (75 mL). The reaction mixture was stirred for 5 h at RT and terminated by evaporation to dryness to yellow–green crystals. H_2O

(50 mL) and EtOAc (50 mL) were added and the phases separated. The aqueous phase was further extracted with EtOAc (2×30 mL). The combined organic phases were washed with H_2O (15 mL), 1 M NaOH (2×15 mL), and H_2O (15 mL). Drying (Na_2SO_4) and evaporation afforded crude **18**. Preparative HPLC (H_2O/MeCN gradient/0.1% TFA) using a Luna $C_{18}(2)$ column (250 mm×21.2 mm, 5 μm) afforded **18**. Compound **18** was dried in vacuo and obtained as brown crystals (2.22 g, 87%); mp: 185–187 °C (dec); ^{1}H NMR ([D$_6$]DMSO): δ = 7.65 (d, J = 8.7 Hz, 4H), 7.71 (s, 4H), 8.74 ppm (bs, 4H); ^{13}C NMR ($CDCl_3$/[D$_6$]DMSO 1:1): δ = 88.6, 94.3, 122.3, 126.0, 128.5, 132.1, 148.3 ppm; HRMS (ESP+) calcd: 281.1079 ($C_{20}H_{13}N_2$ M+1), found: 281.1071; Anal. CHN for $C_{20}H_{12}N_2$·2 TFA·1 H_2O.

1,3-Bis(pyridin-2-ylethynyl)benzene (19); method a: $PdCl_2(PPh_3)_2$ (80 mg, 0.11 mmol) and CuI (22 mg, 0.11 mmol) were suspended in dry CH_2Cl_2 (20 mL) and 1,3-diiodobenzene (750 mg, 2.3 mmol) was added. The mixture was stirred for 5 min at RT before the addition of 2-ethynylpyridine (0.58 mL, 5.7 mmol) and Et_3N (20 mL). The reaction mixture was held at reflux overnight, and terminated by evaporation to dryness. H_2O (50 mL) and EtOAc (50 mL) were added and the phases separated. The aqueous phase was further extracted with EtOAc (2×30 mL). The combined organic phases were washed with H_2O (30 mL), 1 M NaOH (2×30 mL), and H_2O (30 mL), and afterward dried (Na_2SO_4). CF using heptane/EtOAc gradient ($R_{f(\text{heptane/EtOAc 3:2})}$ = 0.17) afforded **19**. Preparative LC–MS (H_2O (0.1% TFA)/MeCN gradient) using a Luna $C_{18}(2)$ column (250 mm×21.2 mm, 5 μm) afforded **19** when fractions were collected on the basis of m/z = 280. Compound **19** was obtained as dark-brown crystals (610 mg, 96%); mp: 187.6–188.9 °C; ^{1}H NMR (CD_3OD): δ = 7.28 (t, J = 6.5 Hz, 2H), 7.39 (t, J = 7.5 Hz, 1H), 7.55 (d, J = 6.0 Hz, 2H), 7.59 (d, J = 7.5 Hz, 2H), 7.69 (t, J = 7.1 Hz, 2H), 7.80 (s, 1H), 8.69 ppm (d, J = 4.9 Hz, 2H); ^{13}C NMR (CD_3OD): δ = 87.1, 90.6, 122.7, 124.7, 128.7, 129.6, 133.3, 135.3, 138.3, 141.2, 148.5 ppm; GC–MS (CI) 280; HRMS (ESP+) calcd: 281.1079 ($C_{20}H_{13}N_2$ M+1), found: 281.1070; Anal. CHN for $C_{20}H_{12}N_2$·$^1/_2$ TFA.

1,3-Bis(pyridin-2-ylethynyl)benzene (19); method b: Into a vial containing a degassed suspension of 1,3-diethynylbenzene (100 mg, 1 mmol), bromobenzene (200 mg, 1 mmol), 2-iodopyridine (205 mg, 1 mmol) and Et_3N (5 mL, 40 mmol), CuI (20 mg, 0.1 mmol) and $PdCl_2(PPh_3)_2$ (40 mg, 0.05 mmol) were added. After stirring at RT for 16 h, the mixture was filtered through Celite, and the Celite was washed with MeOH (5 mL). Concentration in vacuo followed by purification on a reversed-phase liquid chromatography/mass spectrometry (RP HPLC–MS) system afforded **19** (8 mg, 3%); ^{1}H NMR (400 MHz, $CDCl_3$): δ = 7.24–7.28 (m, 2H), 7.37 (t, J = 7.8 Hz, 1H), 7.53–7.55 (m, 2H), 7.58–7.62 (m, 2H), 7.70 (td, J = 7.8, 1.8 Hz, 2H), 7.81–7.84 (m, 1H), 8.62–8.65 ppm (m, 2H); MS m/z: 280.9 $[M+1]^+$.

1,3-Bis(pyridin-3-ylethynyl)benzene (20); method a: 1,3-Diethynylbenzene (0.32 mL 2.4 mmol), 3-iodopyridine (1.46 g, 7.1 mmol), $PdCl_2(PPh_3)_2$ (33 mg, 0.05 mmol), Cs_2CO_3 (2.71 g, 8.3 mmol), and CuI (23 mg, 0.12 mmol) were suspended in dry DMF (6 mL), and the reaction mixture was stirred at 50 °C for two days. H_2O (50 mL) and EtOAc (50 mL) were added and the phases separated. The aqueous phase was further extracted with EtOAc (2×30 mL). The combined organic phases were washed with H_2O (30 mL), 1 M NaOH (2×30 mL), and H_2O (30 mL). Drying (Na_2SO_4) and evaporation afforded crude **20**. Preparative HPLC (H_2O/MeCN gradient (0–18%)/0.1% TFA) using a Luna $C_{18}(2)$ column (250 mm×21.20 mm, 5 μm) gave **20**. TFA residing from HPLC was removed by dissolving **20** in MeOH and run through a SPE-PL-HCO_3 (MP) tube. Compound **20** was obtained as brown crystals (640 mg, 96%); mp: 66.8–67.4 °C; ^{1}H NMR ($CDCl_3$/TMS): δ = 7.31 (dd, J = 4.9, 7.5 Hz, 2H), 7.39 (t, J = 7.5 Hz, 1H), 7.55 (d, J = 7.4 Hz, 2H), 7.76 (s, 1H), 7.83 (d, J = 7.6 Hz, 2H), 8.58 (d, J = 5.1 Hz, 2H), 8.77 ppm (s, 2H); ^{13}C NMR ($CDCl_3$/TMS): δ = 86.7, 91.6, 120.1, 123.0, 123.1, 128.7, 131.8, 134.7, 138.5, 148.8, 152.3 ppm; MS (EI) 280; Anal. CHN for $C_{20}H_{12}N_2$.

1,3-Bis(pyridin-3-ylethynyl)benzene (20); method b: Into a vial containing a degassed suspension of 1,3-diethynylbenzene (100 mg, 1 mmol), bromobenzene (200 mg, 1 mmol), 3-iodopyridine (205 mg, 1 mmol) and Et_3N (5 mL, 40 mmol), CuI (20 mg, 0.1 mmol) and $PdCl_2(PPh_3)_2$ (40 mg, 0.05 mmol) were added. After stirring at RT for 16 h the mixture was filtered through Celite, and the Celite was washed with MeOH (5 mL). Concentration in vacuo followed by purification on an RP HPLC–MS system afforded **20** (30 mg, 10%); ^{1}H NMR (400 MHz, $CDCl_3$): δ = 7.27–7.40 (m, 3H), 7.51–7.56 (m, 2H), 7.74–7.75 (m, 1H), 7.79–7.83 (m, 2H), 8.58 (bs, 2H), 8.78 ppm (bs, 2H); MS m/z: 280.9 $[M+1]^+$.

1,3-Bis(pyridin-4-ylethynyl)benzene (21): $PdCl_2(PPh_3)_2$ (557 mg, 0.73 mmol), CuI (151 mg, 0.73 mmol) and Et_3N (8.3 mL) were suspended in dry THF (20 mL). 1,3-Diethynylbenzene (1.05 mL, 7.9 mmol) and 4-bromopyridine hydrochloride (3.85 g, 19.8 mmol) were suspended in dry THF (10 mL), and added to the former suspension. The reaction mixture was stirred at RT for 1.5 h and then heated at 50 °C for 4.5 h with monitoring by GC–MS. The reaction mixture was filtered through Celite, and the Celite was washed with EtOAc (5 mL). Et_2O (15 mL) was added to the filtrate and the HCl salt was precipitated by addition of saturated HCl in MeOH. The HCl salt of **21** was filtered off and dried carefully under vacuum (2.1 g, 56%); mp: >200 °C (dec). Compound **21** is volatile and should be followed by MS (API-ES+ or EI) or NMR when subjected to heat or vacuum; ^{1}H NMR (CD_3OD): δ = 7.64 (t, J = 6.8 Hz, 1H), 7.86 (dd, J = 2.4, 9.2 Hz, 2H), 8.04 (s, 1H), 8.21 (d, J = 9.6 Hz, 4H), 8.87 ppm (d, J = 9.8 Hz, 4H); ^{13}C NMR ($CDCl_3$/TMS): δ = 87.5, 92.6, 122.7, 128.5, 128.8, 131.9, 133.0, 135.1, 149.8 ppm; HRMS (ESP+) calcd: 281.1079 ($C_{20}H_{13}N_2$ M+1), found: 281.1085 (using MeCN proved vital for obtaining HRMS); Anal. CHN $C_{20}H_{12}N_2$·0.05 PPh_3O·5.5 HCl.

4,4′-Bis(pyridine-2-ylethynyl)biphenyl (22): K_2CO_3 (750 mg, 5.4 mmol) and PPh_3 (33 mg, 0.11 mmol), were added to a solution of **34** (331 mg, 1.1 mmol) in 1,4-dioxane (30 mL) and stirred for 15 min. $PdCl_2(PPh_3)_2$ (76 mg, 0.11 mmol), **40** (394 mg, 1.36 mmol) and H_2O (30 mL) were added, and the reaction mixture was heated at 80 °C for 14 h. H_2O (100 mL) was added and the mixture was extracted with EtOAc (2×75 mL) and CH_2Cl_2 (2×75 mL). The combined organic phases were washed with H_2O (15 mL), 1 M NaOH (15 mL), and H_2O (15 mL). Drying (Na_2SO_4) and evaporation afforded crude **22**. Preparative HPLC (H_2O/MeCN gradient/0.1% TFA) using a Phenomenex Gemini C_6-phenyl 110A column (250 mm×30 mm, 5 μm) gave **22** as sticky brown crystals, which were dried in vacuo (240 mg, 62%); ^{1}H NMR ($CDCl_3$/TMS): δ = 7.47 (d, J = 13.1 Hz, 2H), 7.51 (dt, J = 3.6, 9.8 Hz, 2H), 7.59–7.67 (m, 2H), 7.72 (t, J = 11.9 Hz, 2H), 7.78 (d, J = 13.1 Hz, 2H), 7.82–7.86 (m, 2H), 8.20 (t, J = 10.8 Hz, 2H), 8.84 ppm (t, J = 5.0 Hz, 2H); ^{13}C NMR ($CDCl_3$/TMS): δ = 83.2, 97.8, 126.6, 128.8, 132.3, 132.7, 133.8, 138.0, 142.6, 144.6, 160.1 ppm; Anal. CHN for $C_{26}H_{16}N_2$·3.7 TFA.

4,4′-Bis(pyridine-3-ylethynyl)biphenyl (23): Compound **23** was prepared as light-green crystals (358 mg, 85%); mp: 179.8–181.0 °C, in analogy to the procedure described for **22**. As starting materials, **35** (361 mg, 1.18 mmol) and **41** (431 mg, 1.48 mmol) were used; ^{1}H NMR ([D$_6$]DMSO): δ = 7.53–7.64 (m, 10H), 8.08 (d, J = 6.8 Hz, 2H), 8.54 (d, J = 7.1 Hz, 2H), 8.83 ppm (s, 2H). ^{13}C NMR ([D$_6$]DMSO): δ = 69.1, 74.3, 115.7, 116.8, 120.9, 126.1, 127.4, 129.2, 131.9, 132.6, 152.0 ppm; MS (CI) 356; HRMS (ESP+) calcd: 357.1392

($C_{26}H_{17}N_2$ $M+1$), found: 357.1356; Anal. CHN for $C_{26}H_{16}N_2 \cdot 3.9\,TFA \cdot 2\,H_2O$.

4,4′-Bis(pyridine-4-ylethynyl)biphenyl (24): Compound **24** was prepared as green crystals (328 mg, 78%); mp: 184–187 °C (dec), in analogy to the procedure described for **22**. As starting materials, **36** (361 mg, 1.18 mmol) and **42** (431 mg, 1.479 mmol) were used; ^{1}H NMR ([D$_6$]DMSO/CDCl$_3$): $\delta = 7.64$ (d, $J = 5.7$ Hz, 4H), 7.83 (d, $J = 8.1$ Hz, 4H), 7.92 (d, $J = 8.1$ Hz, 4H), 8.77 ppm (d, $J = 5.7$ Hz, 4H); ^{13}C NMR ([D$_6$]DMSO/CDCl$_3$): $\delta = 79.9$, 90.5, 124.9, 126.1, 127.8, 132.3, 133.1, 142.8, 150.3 ppm; MS (EI) 356; Anal. CHN for $C_{26}H_{16}N_2 \cdot 5\,TFA \cdot 2\,H_2O$.

3,3′-Bis(pyridine-2-ylethynyl)biphenyl (25): Compound **25** was prepared as green sticky crystals (257 mg, 72%); mp: 159.8–162.3 °C (dec), in analogy to the procedure described for **22**. As starting materials, **31** (215 mg, 0.71 mmol) and **37** (256 mg, 0.88 mmol) were used. The crystals were hygroscopic and turned dark brown upon standing; ^{1}H NMR (CDCl$_3$/TMS): $\delta = 7.47$ (t, $J = 7$ Hz, 2H), 7.54–7.62 (m, 6H), 7.67–7.73 (m, 4H), 7.88 (s, 2H), 8.63 ppm (d, $J = 5$ Hz, 2H); ^{13}C NMR ([D$_6$]DMSO): $\delta = 82.6$, 98.8, 120.9, 124.5, 128.9, 129.2, 129.4, 131.2, 131.8, 138.2, 140.5, 142.5, 144.6 ppm; HRMS (ESP+) calcd: 357.1392 ($C_{26}H_{17}N_2$ $M+1$), found: 357.1384; Anal. CHN for $C_{26}H_{16}N_2 \cdot 3\,TFA \cdot 2\,H_2O \cdot 0.05\,PPh_3O$.

3,3′-Bis(pyridine-3-ylethynyl)biphenyl (26): Compound **26** was prepared as light-brown crystals (225 mg, 66%); mp: 145.6–146.3 °C, in analogy to the procedure described for **22**. As starting materials, **32** (293 mg, 0.96 mmol) and **38** (349 mg, 1.2 mmol) were used. Compound **26** was purified on preparative LC–MS (H_2O(0.1% TFA)/MeCN gradient) using a Luna C_{18}(2) (250 mm × 21.20 mm, 5 μm). Fractions were collected on the basis of $m/z = 356$; ^{1}H NMR (CDCl$_3$/TMS): $\delta = 7.46$ (d, $J = 7.5$ Hz, 2H), 7.53 (td, $J = 1.5$, 7.8 Hz, 2H), 7.58–7.61 (m, 2H), 7.61–7.62 (m, 2H), 7.76 (t, $J = 1.2$ Hz, 2H), 8.13 (td, $J = 1.5$, 8.4 Hz, 2H), 8.61 (dd, $J = 1.5$, 5.1 Hz, 2H), 8.89 ppm (d, $J = 1.5$ Hz, 2H); ^{13}C NMR (CD$_3$OD): $\delta = 88.2$, 95.8, 124.3, 126.1, 127.2, 130.8, 132.3, 133.1, 133.9, 143.1, 143.7, 150.5, 153.8 ppm; HRMS (ESP+) calcd: 357.1392 $[M+1]^+$ found: 357.1375; Anal. CHN for $C_{26}H_{16}N_2 \cdot 2\,TFA \cdot 1\,H_2O$.

3,3′-Bis(pyridine-4-ylethynyl)biphenyl (27): Compound **27** was prepared as light-green crystals (221 mg, 88%); mp: 124.0–125.1 °C, in analogy to the procedure described for **27**. As starting materials, **33** (215 mg, 0.71 mmol) and **39** (256 mg, 0.881 mmol) were used; ^{1}H NMR (CD$_3$OD): $\delta = 7.42$ (t, $J = 7.8$ Hz, 2H), 7.82–7.87 (m, 4H), 8.06 (d, $J = 7.5$ Hz, 2H), 8.22–8.28 ppm (m, 4H), 8.99 (d, $J = 6$ Hz, 4H); ^{13}C NMR (CDCl$_3$): $\delta = 86.1$, 93.6, 112.0, 122.8, 128.7, 128.8, 130.5, 131.6, 139.9, 140.9, 142.9 ppm; HRMS (ESP+) calcd: 357.1392 $[M+1]^+$ found: 357.1381; Anal. CHN for $C_{26}H_{16}N_2 \cdot 5.5\,TFA \cdot 3.3\,H_2O$.

2-((5,5-Dimethyl-1,3,2-dioxaborinan-2-yl)ethynyl)pyridyl (28): Diisopropylamine (7.71 mL, 54.9 mmol) and *n*BuLi (34 mL, 54.5 mmol, 1.6 M in hexane) were added to dry Et$_2$O (200 mL) and cooled to −78 °C. The mixture was stirred for 20 min before B(O*i*Pr)$_3$ (16.5 mL, 72.0 mmol) was added. After another 5 min 2-ethynylpyridine (2.74 mL, 27.2 mmol) dissolved in dry Et$_2$O (14 mL) was added. Extra Et$_2$O (12 mL) was added to secure stirring. The resulting yellow suspension was left stirring at −78 °C for 4 h and the cooling bath was removed. After 15 min AcOH (2.50 mL) and then 2,2-dimethyl-1,3-propanediol (7.49 g, 72.0 mmol) were added. The reaction mixture was left stirring at RT for 3 h. CH_2Cl_2 (1 L) was added, and the mixture washed with saturated $NH_4Cl_{(aq)}$ (300 mL), saturated $NaHCO_{3(aq)}$ (300 mL), and H_2O (300 mL). Drying (Na_2SO_4), filtration and evaporation of solvent afforded **28** as a brown oil (3.97 g, 68%); ^{1}H NMR (CDCl$_3$): $\delta = 0.94$ (s, 6H), 3.22 (s, 2H), 3.54 (s, 2H), 7.28 (dd, $J = 5.3$, 6.7 Hz, 1H), 7.49 (d, $J = 6.5$ Hz, 1H), 7.68 (t, $J = 6.4$ Hz, 1H), 8.60 ppm (d, $J = 4.8$ Hz, 1H); ^{13}C NMR (CDCl$_3$): $\delta = 21.8$, 35.2, 36.7, 71.8, 77.7, 82.9, 123.9, 127.9, 136.7, 142.6, 150.2 ppm.

3-((5,5-Dimethyl-1,3,2-dioxaborinan-2-yl)ethynyl)pyridyl (29): Compound **29** was prepared as a yellow (semi)crystalline substance (3.20 g, 59%) in analogy to the procedure described for **28** using 3-ethynylpyridine (2.60 g, 25.2 mmol). No extra Et$_2$O was needed for proper stirring; ^{1}H NMR (CDCl$_3$): $\delta = 0.93$ (s, 6H), 3.25 (s, 2H), 3.52 (s, 2H), 7.25–7.28 (m, 1H), 7.77 (d, $J = 7.1$ Hz, 1H), 8.55 (d, $J = 4.8$ Hz, 1H), 8.72 ppm (s, 1H); ^{13}C NMR (CDCl$_3$): $\delta = 21.7$, 72.3, 77.6, 81.3, 123.9, 139.9, 149.1, 152.7 ppm.

4-((5,5-Dimethyl-1,3,2-dioxaborinan-2-yl)ethynyl)pyridyl (30): Compound **30** was prepared as a dark oil (4.02 g, 58%) in analogy to the procedure described for **28** using 4-ethynylpyridine hydrochloride (4.50 g, 32.2 mmol); ^{1}H NMR (CDCl$_3$): $\delta = 0.91$ (s, 6H), 3.34 (s, 2H), 3.48 (s, 2H), 7.37 (d, $J = 6.2$ Hz, 2H), 8.59 ppm (d, $J = 6.1$ Hz, 2H); ^{13}C NMR (CDCl$_3$): $\delta = 21.7$, 21.9, 32.8, 72.4, 75.1, 82.3, 86.3, 122.0, 123.8, 150.6 ppm.

2-((3-Iodophenyl)ethynyl)pyridine (31): Compound **31** (1.12 g, 81%); mp: 74.9–75.4 °C, was prepared as brown crystals, in analogy to the procedure described for **34** using 1,3-diiodobenzene (1.5 g, 4.5 mmol) and 2-ethynylpyridine (0.56 mL, 5.5 mmol). The reaction mixture was stirred at 35 °C overnight; ^{1}H NMR (CDCl$_3$/TMS): $\delta = 7.10$ (t, $J = 7.0$ Hz, 1H), 7.31–7.38 (m, 1H), 7.51–7.59 (m, 2H), 7.66–7.72 (m, 2H), 7.97 (s, 1H), 8.65 ppm (d, $J = 4.9$ Hz, 1H); ^{13}C NMR (CDCl$_3$/TMS): $\delta = 90.0$, 95.9, 100.1, 121.8, 123.3, 129.5, 130.1, 130.9, 138.0, 138.6, 140.4, 149.0, 152.4 ppm; MS (EI) 305.

3-((3-Iodophenyl)ethynyl)pyridine (32): Compound **32** (1.52 g, 82%); mp: 84.0–84.4 °C, was prepared as yellow–brown crystals in analogy to the procedure described for **34** using 1,3-diiodobenzene (2.0 g, 6.1 mmol) and 3-ethynylpyridine (750 mg, 7.3 mmol). The reaction mixture was stirred at 35 °C overnight; ^{1}H NMR (CDCl$_3$/TMS): $\delta = 7.11$ (t, $J = 7.4$ Hz, 1H), 7.27–7.30 (m, 1H), 7.49 (d, $J = 7.5$ Hz, 1H), 7.70 (d, $J = 7.6$ Hz, 1H), 7.79 (d, $J = 7.5$ Hz, 1H), 7.91 (s, 1H), 8.56 (d, $J = 5.3$ Hz, 1H), 8.75 ppm (s, 1H); ^{13}C NMR (CDCl$_3$/TMS): $\delta = 87.1$, 90.7, 93.6, 119.9, 123.0, 124.5, 129.9, 130.7, 137.7, 138.4, 140.1, 148.8, 152.2 ppm; MS (EI) 305.

4-((3-Iodophenyl)ethynyl)pyridine (33): Compound **33** (2.15 g, 78%) was prepared as a semicrystalline substance in analogy to the procedure described for **34** using 1,3-diiodobenzene (3.0 g, 9.1 mmol) and 4-ethynylpyridine hydrochloride (1.33 g, 9.5 mmol); ^{1}H NMR (CDCl$_3$/TMS): $\delta = 7.12$ (t, $J = 7.8$ Hz, 1H), 7.38 (dd, $J = 1.1$, 5.1 Hz, 2H), 7.52 (d, $J = 7.2$ Hz, 1H), 7.73 (td, $J = 0.9$, 7.8 Hz, 1H), 7.92 (t, $J = 1.1$ Hz, 1H), 8.63 ppm (dd, $J = 1.1$, 5.1 Hz, 2H); ^{13}C NMR (CDCl$_3$/TMS): $\delta = 79.4$, 87.8, 116.9, 125.5, 126.2, 130.0, 131.0, 136.7, 138.2, 140.4, 149.8 ppm; MS (EI) 305.

2-((4-Iodophenyl)ethynyl)pyridine (34): $PdCl_2(PPh_3)_2$ (0319 mg, 0.46 mmol) and CuI (87 mg, 0.46 mmol) were suspended in dry CH_2Cl_2 (75 mL) and 1,4-diiodobenzene (3.0 g, 9.1 mmol) was added. The mixture was stirred for 5 min at RT before the addition of 2-ethynylpyridine (1.10 mL, 11 mmol) and Et$_3$N (75 mL). The reaction mixture was stirred overnight at RT and terminated by evaporation to dryness. CF (heptane/EtOAc gradient) afforded pure **34** as light-brown crystals, which were dried in vacuo (1.55 g, 57%); mp: 82.5–83.5 °C, ^{1}H NMR (CDCl$_3$/TMS): $\delta = 7.30$–7.35 (m, 3H), 7.53 (d, $J = 7.5$ Hz, 1H), 7.67–7.74 (m, 3H), 8.63 ppm (d, $J = 6.3$ Hz, 1H); ^{13}C NMR (CDCl$_3$/TMS): $\delta = 88.4$, 89.8, 95.2, 121.7, 123.0, 127.2, 133.5, 136.3, 137.6, 143.1, 150.1 ppm; MS (EI) 305.

3-((4-Iodophenyl)ethynyl)pyridine (35): Compound **35** (887 mg, 32%); mp: 134.0–134.5 °C, was prepared as yellow crystals, in analogy to the procedure described for **34** using 1,4-diiodobenzene (3.0 g, 9.1 mmol) and 3-ethynylpyridine (1.13 g, 10.9 mmol); ^{1}H NMR ($CDCl_3$/TMS): δ = 7.23–7.32 (m, 3H), 7.72 (d, J = 6.4 Hz, 2H), 7.82 (d, J = 8.0 Hz, 1H), 8.58 (d, J = 4.9 Hz, 1H), 8.78 ppm (s, 1H); ^{13}C NMR ($CDCl_3$/TMS): δ = 87.2, 91.8, 94.9, 116.9, 122.0, 123.1, 133.1, 137.7, 138.6, 148.6, 152.0 ppm; MS (EI) 305.

4-((4-Iodophenyl)ethynyl)pyridine (36): Compound **36** (1.75 g, 63%) was prepared as sticky yellow–brown crystals in analogy to the procedure described for **34** using 1,4-diiodobenzene (3.0 g, 9.1 mmol) and 4-ethynylpyridine hydrochloride (1.33 g, 9.5 mmol); ^{1}H NMR ($CDCl_3$): δ = 7.31 (d, J = 6.4 Hz, 2H), 7.62 (d, J = 4.8 Hz, 2H), 7.69 (d, J = 6.5 Hz, 2H), 8.25 ppm (d, J = 4.8 Hz, 2H), ^{13}C NMR ($CDCl_3$/TMS): δ = 87.9, 93.0, 95.5, 121.6, 125.5, 126.2, 133.3, 137.7, 149.8 ppm; MS (EI) 305.

2-((3-(5,5-Dimethyl-1,3,2-dioxaborinan-2-yl)phenyl)ethynyl)pyridine (37): Compound **37** (352 mg, 91%) was prepared as a red–brown semicrystalline substance in analogy to the procedure described for **40** using **31** (300 mg, 0.98 mmol); ^{1}H NMR ($CDCl_3$/TMS): δ = 1.02 (s, 6H), 3.79 (s, 4H), 7.28–733 (m, 1H), 7.37 (d, J = 6.2 Hz, 1H), 7.54 (d, J = 8.1 Hz, 1H), 7.65–7.75 (m, 2H), 7.80 (d, J = 7.9 Hz, 1H), 8.07 (s, 1H), 8.63 ppm (d, J = 5.0 Hz, 1H).

3-((3-(5,5-Dimethyl-1,3,2-dioxaborinan-2-yl)phenyl)ethynyl)pyridine (38): Compound **38** (352 mg, 96%) was prepared as a red semicrystalline substance in analogy to the procedure described for **40** using a solution of **32** (386 mg, 1.27 mmol); ^{1}H NMR ($CDCl_3$/TMS): δ = 0.98 (s, 3H), 104 (s, 3H), 3.59 (s, 2H), 3.78 (s, 2H), 7.39 (t, J = 7.0 Hz, 1H), 7.60–7.67 (m, 2H), 7.86 (d, J = 7.9 Hz, 1H), 8.02 (s, 1H), 8.15 (d, J = 7.2 Hz, 1H), 8.60 (d, J = 4.8 Hz, 1H), 8.77 ppm (s, 1H).

4-((3-(5,5-Dimethyl-1,3,2-dioxaborinan-2-yl)phenyl)ethynyl)pyridine (39): Compound **39** (295 mg, 81%) was prepared in analogy to the procedure described for **40** using **33** (383 mg, 1.26 mmol); ^{1}H NMR ($CDCl_3$/TMS): δ = 1.04 (s, 6H), 3.79 (s, 4H), 7.35–7.40 (m, 3H), 7.60 (d, J = 7.6 Hz, 1H), 7.81 (d, J = 7.6 Hz, 1H), 8.01 (s, 1H), 8.59 ppm (d, J = 6.1 Hz, 2H); ^{13}C NMR ($CDCl_3$/TMS): δ = 21.9, 31.9, 72.0, 72.4, 77.7, 121.4, 125.6, 127.7, 128.5, 131.8, 133.8, 134.5, 137.6, 149.7 ppm.

2-((4-(5,5-Dimethyl-1,3,2-dioxaborinan-2-yl)phenyl)ethynyl)pyridine (40): A solution of **34** (350 mg, 1.15 mmol) in dry Et_2O (10 mL) was cooled to −78 °C. *n*BuLi (1.54 mL, 2.3 mmol, 1.49 M in hexane) was added dropwise and the mixture was left stirring for 10 min before addition of $B(OiPr)_3$ (0.70 mL, 3.0 mmol) dissolved in dry Et_2O (6 mL). After 3.5 h at −78 °C the cooling bath was removed and after 15 min AcOH (0.011 mL) and then 2,2-dimethyl-1,3-propanediol (299 mg, 2.9 mmol) were added. The reaction mixture was stirred overnight at RT. CH_2Cl_2 (50 mL) was added and the mixture washed with saturated $NH_4Cl_{(aq)}$ (15 mL), saturated $NaHCO_{3(aq)}$ (15 mL) and H_2O (15 mL). Drying (Na_2SO_4), filtration and evaporation afforded **40** (331 mg, 99%); ^{1}H NMR ($CDCl_3$/TMS): δ = 1.03 (s, 6H), 3.79 (s, 4H), 7.24–7.29 (m, 1H), 7.35–7.39 (m, 1H), 7.52 (d, J = 6.9 Hz, 1H), 7.58 (d, J = 7.0 Hz, 1H), 7.63–7.71 (m, 1H), 7.78 (d, J = 7.0 Hz, 2H), 8.63 ppm (d, J = 5.5 Hz, 1H).

3-((4-(5,5-Dimethyl-1,3,2-dioxaborinan-2-yl)phenyl)ethynyl)pyridine (41): Compound **41** (361 mg, 98%) was prepared in analogy to the procedure described for **40** using **35** (386 mg, 1.27 mmol); ^{1}H NMR ($CDCl_3$/TMS): δ = 1.05 (s, 6H), 3.79 (s, 4H), 7.27–7.31 (m, 1H), 7.54 (d, J = 7.4, 2H), 7.72 (d, J = 7.9 Hz, 1H), 7.76–7.83 (m, 2H), 8.53 (d, J = 5.3 Hz, 1H), 8.78 ppm (m, 1H).

4-((4-(5,5-Dimethyl-1,3,2-dioxaborinan-2-yl)phenyl)ethynyl)pyridine (42): Compound **42** (257 mg, 84%) was prepared as a dark-brown semicrystalline substance in analogy to the procedure described for **40** using **36** (320 mg, 1.05 mmol); ^{1}H NMR ($CDCl_3$/TMS): δ = 1.03 (s, 6H), 3.78 (s, 4H), 7.37–7.39 (m, 2H), 7.53 (d, J = 8.1 Hz, 2H), 7.81 (d, J = 8.6 Hz, 2H), 8.61 ppm (bs, 2H); ^{13}C NMR ($CDCl_3$/TMS): δ = 21.8, 35.5, 72.0, 72.4, 77.2, 124.0, 125.6, 130.9, 133.3, 133.8, 137.7, 149.7 ppm.

1,4-Di(pyridine-2-yl)buta-1,3-diyne (43): Purified as a by-product of other palladium-catalyzed cross-couplings. 2-Bromothiazole (0.9 mL, 10 mmol), was dissolved in dry CH_2Cl_2 (20 mL). CuI (20 mg, 0.1 mmol), $PdCl_2(PPh_3)_2$ (72 mg, 0.1 mmol), Et_3N (10 mL), and 2-ethynylpyridine (1.51 mL, 15 mmol) were added, and the reaction mixture was held at reflux for 16 h. The mixture was diluted with EtOAc (60 mL). The mixture was washed with H_2O (100 mL). The EtOAc phase was filtered and evaporated. CF (CH_2Cl_2/Et_3N/MeOH gradient 95:5:0 to 95:5:5) afforded **43** in the first fraction, and **9** in the second fraction obtained. The fractions were evaporated and dried in vacuo to afford **43** (597 mg, 39%) as light-brown crystals. Compound **9** was obtained in 42% with data in agreement with earlier described. **43**: ^{1}H NMR ($CDCl_3$/TMS): δ = 7.25–7.29 (m, 2H), 7.49 (d, J = 7.5 Hz, 2H), 7.67 (dt, J = 2.9, 7.5 Hz, 2H), 8.6 ppm (d, J = 8.0 Hz, 2H) ^{13}C NMR ($CDCl_3$/TMS): δ = 77.2, 82.7, 123.4, 127.5, 136.2, 142.4, 150.1 ppm; MS (EI) 204 $[M]^+$; Anal. CHN for $C_{14}H_8N_2$.

1,4-Di(pyridine-3-yl)buta-1,3-diyne (44): Purified as a by-product of other palladium-catalyzed cross-couplings. 4,4′-Dibromobiphenyl (700 mg, 2.2 mmol) was dissolved in dry CH_2Cl_2 (20 mL). CuI (21 mg, 0.1 mmol), $PdCl_2(PPh_3)_2$ (79 mg, 0.1 mmol), Et_3N (20 mL), and 3-ethynylpyridine (810 mg, 7.9 mmol) were added, and the reaction mixture was held at reflux for 14 h. The mixture was diluted with EtOAc (60 mL), Et_2O (15 mL) was added to precipitate PPh_3O and filtered. The mixture was washed with H_2O (100 mL). The organic phase was dried ($MgSO_4$) and evaporated. CF (heptane/Et_3N/EtOAc 95:5:0 to 95:5:5) afforded **44** as well as unreacted 4,4′-dibromobiphenyl. The fractions holding **44** were evaporated and dried in vacuo to afford **44** as light-grey crystals (589 mg, 73%); mp: 157.0–157.9 °C; ^{1}H NMR ($CDCl_3$/TMS): δ = 7.30 (dd, J = 4.4, 8.0 Hz, 2H), 7.83 (td, J = 1.8, 7.4 Hz, 2H), 8.61 (dd, J = 2.1, 7.1 Hz, 2H), 8.78 ppm (d, J = 1.8 Hz, 2H); ^{13}C NMR ($CDCl_3$/TMS): δ = 76.6, 79.2, 118.9, 123.2, 139.4, 149.7, 153.2 ppm; MS (EI) 204; HRMS (ESP+) calcd: 205.0766 ($C_{14}H_9N_2$ M+1), found: 205.0765; Anal. CHN for $C_{14}H_8N_2$·3 TFA·2.5 H_2O.

1,4-Di(pyridine-4-yl)buta-1,3-diyne (45): Purified as a by-product of other palladium-catalyzed cross-couplings. 2,5-Dibromothiazole (250 mg, 1.0 mmol), 4-ethynylpyridine hydrochloride (359 mg, 2.6 mmol), $Pd(PtBu_3)_2$ (21 mg, 0.04 mmol), $Pd_2(dba)_3$ (38 mg, 0.04 mmol), and CuI (18 mg, 0.09 mmol) were dissolved in 1,4-dioxane (5 mL). Cy_2NMe (2.2 mL, 10.3 mmol) was added and the reaction mixture was heated at 60 °C for two days. The mixture was diluted with Et_2O (3 mL), and filtered through Decalite. The Decalite was washed with cold EtOAc (10 mL). The combined organic filtrates were concentrated in vacuo to afford crude product. CF (heptane/Et_3N/EtOAc 95:5:0 to 95:5:10) afforded **45** as well as number of unidentified products in smaller amounts. The fractions holding **45** were evaporated, and dried in vacuo to afford **45** as brown crystals (64 mg, 24%); mp: >200 °C (dec); ^{1}H NMR ([D_6]DMSO): δ = 7.60–7.68 (m, 4H), 8.75 ppm (bs, 4H); ^{13}C NMR ([D_6]DMSO): δ = 77.2, 80.2, 126.2, 150.0 ppm; MS (EI) 204; HRMS (ESP+) calcd: 205.0766 ($C_{14}H_9N_2$ M+1), found: 205.0765; Anal. CHN for $C_{14}H_8N_2$·0.5 HCl.

Pharmacology

Materials: All cell culture reagents were obtained from Gibco unless otherwise stated.

Inhibition of forskolin-stimulated cAMP production: CHO cells expressing mGluR2 or mGluR4 (previously described by Tanabe et al.)[11] were cultured in DMEM with GlutaMAX-I with 10% dialyzed FBS, 1% penicillin–streptomycin, and L-proline (2.5 g L^{-1}) at 5% CO_2 at 37 °C. Cells were seeded at 26000 cells per well (96-well plate) 24 h before assaying. Cells were washed with DPBS prior to compound addition. For agonist testing cells were first incubated with cAMP-ground buffer (DPBS with 1 mM $CaCl_2$, 1 mM $MgCl_2$ and 1 mM IBMX) for 20 min at 37 °C. The buffer was then replaced with test compounds diluted in cAMP-ground buffer supplemented with 25 μM forskolin and incubated at 37 °C for 10 min. For antagonist testing cells were first incubated with test compounds diluted in cAMP-ground buffer for 20 min at 37 °C, and then replaced with cAMP-ground buffer containing test compounds, 25 μM forskolin, and L-glutamate corresponding to the EC_{80} (20 μM for mGluR2, 30 μM for mGluR4) for 10 min at 37 °C. All reactions were terminated by aspiration and addition of ice-cold sodium acetate buffer pH 6.2 supplemented with 0.1% Triton X-100 and 0.1 mM IBMX. cAMP levels were quantified using the Adenylyl Cyclase Activation FlashPlate Assay (PerkinElmer) and interpolated from a cAMP standard curve.

Inositol phosphate (IP) turnover assay: CHO cells expressing the mGluR1 (previously described by Aramori and Nakanishi)[10] were cultured as described in the cAMP assay above. Cells were seeded at 26000 cells per well (96-well plate) and labeled with myo-[2-^{3}H]inositol (4 μCi mL^{-1}, TRK911, GE Healthcare) 24 h before assaying. Prior to compound addition cells were washed with DPBS. For agonist testing cells were first incubated with IP-ground buffer (HBSS containing 20 mM HEPES, 1 mM $CaCl_2$, 1 mM $MgCl_2$ and 0.85 mg mL^{-1} LiCl, pH 7.4) for 30 min at 37 °C. The buffer was then replaced with test compounds diluted in IP-ground buffer and incubated at 37 °C for 30 min. For antagonist testing cells were first incubated with test compounds diluted in IP-ground buffer for 30 min at 37 °C, and then replaced with IP-ground buffer containing test compounds and 30 μM L-glutamate corresponding to the EC_{80} for 30 min at 37 °C. All reactions were terminated by aspiration and addition of ice-cold 10 mM formic acid and incubation for 30 min at 4 °C. Yttrium silicate scintillation proximity assay beads (RPNQ0010, GE Healthcare) were used for measuring radioactivity from generated [^{3}H]IP as previously described (Brandish et al.).[21] Radioactivity was quantified in a Packard TopCount microplate scintillation counter and responses were read as counts per minute (CPM). All experiments were performed in triplicate and repeated in at least two independent experiments.

Intracellular Ca^{2+} measurements (test of 19–21 on mGluR1): CHO cells expressing mGluR1 were cultured as described for the cAMP assay. Cells were seeded at 30000 cells per well in flat clear-bottom black microplates (96-well format) the day before the assay. Cells were washed with DPBS before loading with dye. The dye loading solution (Fluo-4 NW Calcium Assay Kit, F36206, Molecular Probes) was prepared according to the manufacturer's instructions by dissolving it in HEPES buffer (1× HBSS supplemented with 1 mM $MgCl_2$, 1 mM $CaCl_2$, 20 mM HEPES, pH 7.4) supplemented with 2.5 mM probenecid; 50 μL dye loading solution was added to each well. Cells were incubated with the dye for 60 min at 37 °C, after which they were washed with HEPES buffer supplemented with 2.5 mM probenecid. For agonist testing, cells were incubated with HEPES buffer supplemented with 2.5 mM probenecid for 30 min at RT followed by measurement on a NOVOstar instrument (BMG Labtech). Test compounds were diluted in HEPES buffer and added automatically after baseline measurements. For antagonist testing cells were incubated with the test compound diluted in HEPES buffer supplemented with 2.5 mM probenecid for 30 min at RT before measurement by NOVOstar. Cells were stimulated using 15 μM Glu, corresponding to EC_{80}, diluted in HEPES buffer. Glu was added automatically after baseline measurements. For the fluorescent measurements on the NOVOstar instrument an excitation filter at 485 nm and an emission filter at 520 nm were used. Data originate from three independent experiments (duplicate measurements).

Modeling

Protein sequence alignment of the TM helices of Family A–C GPCRs and homology model of mGluR5

mGluR5 belongs to Family C of GPCRs, and because there are no crystal structures available of the TM region of this family, we decided to use two Family A GPCR crystal structures as templates for construction of our homology model. Mutational studies have indicated that the binding site for negative allosteric mGluR5 modulators is located between the upper halves of the seven TM helices[5a] and thus an alignment of only the helices was used for model building. In both templates the second extracellular loop (ECL2) between TM4 and 5 is, to some extent, involved in ligand binding, but significantly different in structure and length. However, ECL2 of mGluR5 does not match any of the templates in length or sequence, making modeling of this loop extremely difficult. Therefore, we decided to exclude ECL2 from homology modeling. The two other extracellular loops (between TM2 and 3 and between TM6 and 7) are shorter than in the templates and were included to constrain the distances between the helices in the mGluR5 model. To obtain a reliable sequence alignment between the TM helices of mGluR5 and the two templates, an alignment was created of all Family A, B, and C GPCRs as described below.

Sequences for Family A, B, and C GPCRs were retrieved from previous studies,[22] and the entry numbers given below refer hereto. First, a joint ungapped alignment was produced for the seven TM helices of all human Family A GPCRs in MEGA4.[23] The alignment was anchored on the conserved Family A residues used in the Ballesteros–Weinstein indexing system.[24] Second, human Family B and C GPCRs were aligned to the Family A receptor alignment, again by anchoring on conserved residues, but to a lesser extent those from the Ballesteros–Weinstein indexing and to a larger extent depending on sequence conservation in a large number or receptor homologues and orthologues.[25] For example, the TM3 alignment was anchored on the cysteine that forms the disulfide bond to ECL2 because this residue is more conserved than R3.50 in Families B and C. Third, the alignment of the human mGluR5 (entry: P41594) to the human β2-adrenergic and adenosine A_{2A} receptors (entries: P07550 and P29274, respectively) was extracted from the overall alignment, and the TM2–3 and TM6–7 loops were added in the mGluR5 sequence.

The human mGluR5 homology model was constructed with MODELLER,[26] version 9v8 using the human β2-adrenergic and adenosine A_{2A} receptor crystal structures as templates and the alignment presented in the Supporting Information. The template structures (PDB IDs: 2RH1[14] and 3EML[15]) were retrieved from the RCSB Protein Data Bank[27] (http://www.rcsb.org/), and all residues that are not part of the TM helices were deleted. α-Helical restraints were

added to TM2, TM6, and TM7 to prevent the short extracellular TM2–3 and TM6–7 loops from distorting the helical structure; 100 models were constructed using the "slow" MD refinement level and default settings otherwise. The models were assessed with the discrete optimized protein energy potential[28] (DOPE) incorporated in MODELLER, and the best scoring model was selected for further studies.

Ligand docking

Maestro[29] of the Schrödinger Suite 2010 version was used to build compound **19** and add hydrogen atoms to the mGluR5 model. Docking was performed using Glide.[30] Residues Ile651$^{3.32}$, Pro655$^{3.36}$, and Trp785$^{6.48}$ were used to define the box center of the receptor grid, and the box size was set to 22 Å on each axis. Docking was performed without post-docking minimization asking for 20 output poses, and remaining parameters were set to default. The top-scoring pose of **19** was selected as the most likely binding mode.

Acknowledgements

B.H.K. was supported by the Drug Research Academy, Faculty of Pharmaceutical Sciences, University of Copenhagen. C.M. and H.B.-O. were supported by the Drug Research Academy (Faculty of Pharmaceutical Sciences, University of Copenhagen, Denmark), the A. P. Møller Foundation for the Advancement of Medical Sciences, and the Brødrene Hartmanns Fond. K.H. was supported the Carlsberg Foundation and the Drug Research Academy. D.G. was supported by the Alfred Benzon Foundation. J.M.M. was supported by the Danish Council for Independent Research Medical Sciences and the Lundbeck Foundation.

Keywords: allosteric modulators · cross-coupling · mGluR5 · molecular modeling · structure–activity relationships

[1] a) H. Bräuner-Osborne, J. Egebjerg, E. Ø. Nielsen, U. Madsen, P. Krogsgaard-Larsen, *J. Med. Chem.* **2000**, *43*, 2609 – 2645; b) C. M. Niswender, P. J. Conn, *Annu. Rev. Pharmacol. Toxicol.* **2010**, *50*, 295 – 322; c) S. F. Traynelis, L. P. Wollmuth, C. J. McBain, F. S. Menniti, K. M. Vance, K. K. Ogden, K. B. Hansen, H. Yuan, S. J. Myers, R. Dingledine, *Pharmacol. Rev.* **2010**, *62*, 405 – 496.

[2] a) K. M. Houamed, J. L. Kuijper, T. L. Gilbert, B. A. Haldeman, P. J. O'Hara, E. R. Mulvihill, W. Almers, F. S. Hagen, *Science* **1991**, *252*, 1318 – 1321; b) M. Masu, Y. Tanabe, R. Shigemoto, S. Nakanishi, *Nature* **1991**, *349*, 760 – 765.

[3] a) S. Petersen, C. Bomme, C. Baastrup, A. Kemp, G. R. J. Christoffersen, *Pharmacol. Biochem. Behav.* **2002**, *73*, 381 – 389; b) M. G. Moloney, *Nat. Prod. Rep.* **2002**, *19*, 597 – 616; c) B. Schulz, M. Fendt, F. Gasparini, K. Lingenhöhl, R. Kuhn, M. Koch, *Neuropharmacology* **2001**, *41*, 1 – 7.

[4] a) F. Gasparini, R. Kuhn, J.-P. Pin, *Curr. Opin. Pharmacol.* **2002**, *2*, 43 – 49; b) J. Brodkin, C. Busse, S. J. Sukoff, M. A. Varney, *Pharmacol. Biochem. Behav.* **2002**, *73*, 359 – 366; c) M. J. Marino, P. J. Conn, *Curr. Opin. Pharmacol.* **2006**, *6*, 98 – 102.

[5] a) P. Malherbe, N. Kratochwil, M.-T. Zenner, J. Piussi, C. Diener, C. Kratzeisen, C. Fischer, R. H. P. Porter, *Mol. Pharmacol.* **2003**, *64*, 823 – 832; b) A. Mühlemann, N. A. Ward, N. Kratochwil, C. Diener, C. Fischer, A. Stucki, G. Jaeschke, P. Malherbe, R. H. P. Porter, *Eur. J. Pharmacol.* **2006**, *529*, 95 – 104.

[6] P. Malherbe, N. Kratochwil, A. Muhlemann, M. T. Zenner, C. Fischer, M. Stahl, P. R. Gerber, G. Jaeschke, R. H. Porter, *J. Neurochem.* **2006**, *98*, 601 – 615.

[7] a) M. I. Page, W. P. Jencks, *Nat. Acad. Sci. USA* **1971**, *68*, 1678 – 1683; b) W. P. Jencks, *Proc. Natl. Acad. Sci. USA* **1981**, *78*, 4046 – 4050.

[8] a) A. Christopoulus, M. K. O. Grant, N. Ayoubzadeh, O. N. Kim, P. Sauerberg, L. Jeppesen, E. E. El-Fakahany, *J. Pharmacol. Exp. Ther.* **2001**, *298*, 1260 – 1268; b) J.-L. Soulier, O. Russo, M. Giner, L. Rivail, M. Berthouze, S. Ongeri, B. Maigret, R. Fishmeister, F. Lezoualc'h, S. Sicsic, I. Berque-Bestel, *J. Med. Chem.* **2005**, *48*, 6220 – 6228.

[9] N. D. P. Cosford, L. Tehrani, J. Roppe, E. Schweiger, N. D. Smith, J. Anderson, L. Bristow, J. Brodkin, X. Jiang, I. McDonald, S. Rao, M. Washburn, M. A. Varney, *J. Med. Chem.* **2003**, *46*, 204 – 206.

[10] I. Aramori, S. Nakanishi, *Neuron* **1992**, *8*, 757 – 765.

[11] a) Y. Tanabe, M. Masu, T. Ishii, R. Shigemoto, S. Nakanishi, *Neuron* **1992**, *8*, 169 – 179; b) Y. Tanabe, A. Nomura, M. Masu, R. Shigemoto, N. Mizuno, S. Nakanishi, *J. Neurosci.* **1993**, *13*, 1372 – 1378.

[12] J. M. Mathiesen, N. Svendsen, H. Bräuner-Osborne, C. Thomsen, M. T. Ramirez, *Br. J. Pharmacol.* **2003**, *138*, 1026 – 1030.

[13] M. B. Hermit, J. R. Greenwood, B. Nielsen, L. Bunch, C. G. Jørgensen, H. T. Vestergaard, T. B. Stensbøl, C. Sanchez, P. Krogsgaard-Larsen, U. Madsen, H. Bräuner-Osborne, *Eur. J. Pharmacol.* **2004**, *486*, 241 – 250.

[14] V. Cherezov, D. M. Rosenbaum, M. A. Hanson, S. G. Rasmussen, F. S. Thian, T. S. Kobilka, H. J. Choi, P. Kuhn, W. I. Weis, B. K. Kobilka, R. C. Stevens, *Science* **2007**, *318*, 1258 – 1265.

[15] V. P. Jaakola, M. T. Griffith, M. A. Hanson, V. Cherezov, E. Y. Chien, J. R. Lane, A. P. IJzerman, R. C. Stevens, *Science* **2008**, *322*, 1211 – 1217.

[16] S. Topiol, M. Sabio, *Biochem. Pharmacol.* **2009**, *78*, 11 – 20.

[17] A. Pagano, D. Rüegg, S. Litschig, N. Stoehr, C. Stierlin, M. Heinrich, P. Floersheim, L. Prézeau, F. Carroll, J. P. Pin, A. Cambria, I. Cranesic, P. Flor, F. Gasparini, R. Kuhn, *J. Biol. Chem.* **2000**, *275*, 33750 – 33758.

[18] The PyMOL Molecular Graphics System, version 1.4, Schrödinger LLC, New York, NY (USA), **2011**.

[19] D. R. Coulson, *Inorg. Synth.* **1972**, *13*, 121.

[20] a) J. Suffert, *J. Org. Chem.* **1989**, *54*, 509; b) B. E. Love, E. G. Jones, *J. Org. Chem.* **1999**, *64*, 3755 – 3756; c) H.-S. Lin, L. A. Paquette, *Synth. Commun.* **1994**, *24*, 2503 – 2506.

[21] P. E. Brandish, L. A. Hill, W. Zheng, E. M. Scolnick, *Anal. Biochem.* **2003**, *313*, 311 – 318.

[22] a) R. Fredriksson, D. E. Gloriam, P. J. Hoglund, M. C. Lagerström, H. B. Schiöth, *Biochem. Biophys. Res. Commun.* **2003**, *301*, 725 – 734; b) R. Fredriksson, P. J. Hoglund, D. E. Gloriam, M. C. Lagerström, H. B. Schiöth, *FEBS Lett.* **2003**, *554*, 381 – 388; c) R. Fredriksson, M. C. Lagerström, L. G. Lundin, H. B. Schiöth, *Mol. Pharmacol.* **2003**, *63*, 1256 – 1272; d) D. E. Gloriam, H. B. Schiöth, R. Fredriksson, *Biochim. Biophys. Acta Gen. Subj.* **2005**, *1722*, 235 – 246.

[23] K. Tamura, J. Dudley, M. Nei, S. Kumar, *Mol. Biol. Evol.* **2007**, *24*, 1596 – 1599.

[24] J. A. Ballesteros, H. Weinstein in *Meth. Neurosci., Vol. 25* (Ed.: C. S. Stuart), Academic Press, **1995**, pp. 366 – 428.

[25] a) T. K. Bjarnadóttir, R. Fredriksson, P. J. Hoglund, D. E. Gloriam, M. C. Lagerström, H. B. Schiöth, *Genomics* **2004**, *84*, 23 – 33; b) D. E. Gloriam, T. K. Bjarnadóttir, Y. L. Yan, J. H. Postlethwait, H. B. Schiöth, R. Fredriksson, *Mol. Phylogenet. Evol.* **2005**, *35*, 470 – 482; c) D. E. Gloriam, R. Fredriksson, H. B. Schiöth, *BMC Genomics* **2007**, *8*, 338; d) T. Haitina, R. Fredriksson, S. M. Foord, H. B. Schiöth, D. E. Gloriam, *BMC Genomics* **2009**, *10*, 24; e) M. C. Lagerström, A. R. Hellstrom, D. E. Gloriam, T. P. Larsson, H. B. Schiöth, R. Fredriksson, *PLoS Comput. Biol.* **2006**, *2*, 493 – 507.

[26] A. Sali, T. L. Blundell, *J. Mol. Biol.* **1993**, *234*, 779 – 815.

[27] H. M. Berman, J. Westbrook, Z. Feng, G. Gilliland, T. N. Bhat, H. Weissig, I. N. Shindyalov, P. E. Bourne, *Nucleic Acids Res.* **2000**, *28*, 235 – 242.

[28] M. Y. Shen, A. Sali, *Protein Sci.* **2006**, *15*, 2507 – 2524.

[29] Maestro version 9.1, Schrödinger LLC, New York, NY (USA), **2010**.

[30] Glide version 5.6, Schrödinger LLC, New York, NY (USA), **2010**.

Received: December 7, 2011
Revised: December 21, 2011
Published online on January 20, 2012

